IN VIVO BIOMECHANICAL STRAIN RESPONSE OF THE LAMINA CRIBROSA TO INTRAOCULAR PRESSURE CHANGE AS A RESULT OF GLAUCOMA MEDICATION CHANGE

by

Vanessa Hannay

A thesis submitted to Johns Hopkins University
in conformity with the requirements for the degree of
Master of Science in Engineering

Baltimore, Maryland
December 2022

Abstract

The aim of the present pilot study was to evaluate the feasibility of a method for characterizing the short-term, *in vivo* biomechanical response of the lamina cribrosa (LC) in the eyes of patients starting glaucoma medication as a potential biomarker for primary open angle glaucoma (POAG). Radial optical coherence tomography (OCT) image volumes were acquired and intraocular pressure (IOP) was measured for 23 eyes from 15 patients before starting glaucoma medication and after a duration of 7.3 $\pm$ 1.4 days. Pre- and post-treatment image volumes were compared using digital volume correlation (DVC) to determine the anterior LC (ALC) strains and anterior LC depth (ALD) change. After the one-week treatment period, IOP decrease caused significant tensile E_{zz} greater than baseline error, compressive E_{rr} greater than baseline and correlation error, and small but significant posterior ALD change in Group 1 (eyes which had an IOP decrease of at least 4 mmHg). In Group 2 (eyes with 0-1 mmHg IOP change), there was a significant tensile E_{zz}, however its magnitude was approximately three times smaller than that of the Group 1 eyes and it did not exceed baseline or correlation error. Strain magnitudes were more highly correlated with percent IOP decrease than IOP decrease. Strains did not vary by quadrant of the LC and did not relate to ALD change. ALD change did not increase with increased IOP decrease. Strains and strain compliance increased with decreasing mean deviation (MD) and visual field index (VFI), but decreased with thinner average retinal nerve fiber layer (RNFL). Strains, strain compliance response, ALD change, RNFL, MD, and VFI were not significantly related to patient age. The results of the present study suggest the current method is a promising method for

measuring repeatable LC strains and depth change in the eyes of patients subjected to IOP change as a result of glaucoma medication change.

Primary Reader and Advisor:

Thao D. (Vicky) Nguyen, Professor, Department of Mechanical Engineering and Department of Materials Science, Johns Hopkins University

Secondary Reader:

Harry A. Quigley, Professor of Ophthalmology, Glaucoma Center of Excellence, Johns Hopkins University School of Medicine

Acknowledgments

First and foremost, I would like to thank my PI, Dr. Vicky Nguyen. Thank you for allowing me the opportunity to pursue research with the Nguyen Lab. I did not have a lot of confidence in myself as a researcher when I first entered the lab. Throughout my time in the Nguyen Lab, I have slowly improved my research and analysis skills and am confident I will continue to grow and take the invaluable experiences I have learned here and be able to apply them outside the lab in industry where I hope to work as an R&D engineer. Thank you for believing in me, encouraging me to persevere, and teaching me to become a more critical thinker and better researcher. I am grateful for my time in the Nguyen Lab. It has been a great experience accompanied by great people.

Secondly, I would like to thank Dr. Harry Quigley. Thank you for the opportunity to pursue research at the Wilmer Eye Institute's Glaucoma Center. It has been a privilege to do research with both an expert in glaucoma and a clinician at the Johns Hopkins Medical Center. This research experience has allowed me to grow professionally, expand my perspective, and learn to communicate with patients and clinicians alike. These are all invaluable skills I will take with me to the biomedical engineering industry as I start my professional journey. Thank you for your patience, expertise, and guidance.

There are several other individuals affiliated with Johns Hopkins Medicine and the Wilmer Glaucoma Center whom I would like to acknowledge. Dr. Ian Pitha and Dr. Pradeep Ramulu, thank you both for helping me recruit more patient volunteers for my study and providing your time and support. I would also like to acknowledge my colleague, Rebecca

Mirville, from Meharry Medical School who researched alongside me under Dr. Quigley at the Wilmer Glaucoma Center this summer. Although we only spent a couple months researching together, I enjoyed working with you and wish you the best going forward in medical school. Thank you for providing assistance with imaging for my study.

Next, I would like to acknowledge my colleague Cameron Czerpak from the Nguyen Lab for providing me with imaging assistance, guidance, support, and feedback throughout my time in the lab. Thank you for being patient, always encouraging me, and taking the time to provide me with quality feedback that has allowed me to grow more confident and independent as a researcher. You have been a great mentor and I wish you the best of luck going forward in your goals.

Last but not least, I'd like to acknowledge my family, partner, and close friends. Thank you for supporting my goal of pursuing a graduate degree in engineering. I am grateful I had the opportunity to pursue my master's at Johns Hopkins. Thank you for being positive and encouraging me to stay strong during challenging times. I am grateful to you for believing in me and supporting me in all my endeavors.

Contents

List of Tables

List of Figures

Chapter 1

Introduction

1.1 Glaucoma

Glaucoma is the leading cause of irreversible blindness [1–3]. It is estimated that Primary Open Angle Glaucoma (POAG) affects 58 million people worldwide with the number of cases expected to nearly double by 2040 [4]. Glaucoma is significantly associated with the level of intraocular pressure (IOP), such that the higher the IOP, the more likely retinal ganglion cell (RGC) axons of the optic nerve will be damaged, resulting in irreversible, progressive vision loss if left untreated [3, 5]. Glaucoma may be categorized broadly into open-angle and angle-closure (acute) glaucoma. POAG is the most common form of glaucoma, affecting over 80% of glaucoma patients in the United States [3]. The present study focuses on eyes with POAG since it is the most prevalent form of glaucoma, and its underlying mechanism is less well understood [3]. The severity of POAG can be gauged by several clinical measures including average retinal nerve fiber layer (RNFL) thickness, mean deviation (MD), and visual field index (VFI). A thinner RNFL, more negative mean deviation, and lower visual field index are associated with increased damage and disease progression [6, 7].

Currently, there is no cure for POAG. Vision loss due to glaucoma damage cannot be completely stopped or reversed; however, progression can be slowed. This is best accom-

plished through IOP-lowering treatments [8–10]. Treatment options to reduce IOP in the eyes of glaucoma patients range in invasiveness from topical eye drops to laser procedures to surgical intervention [11, 12]. If detected and managed early, vision loss from glaucoma may be prevented [3]. More often than not, POAG progresses slowly and is asymptomatic prior to vision loss, remaining undetected while damage to the optic nerve accumulates.

1.2 Problem Statement and Aims

The exact mechanism by which IOP level affects vision loss has not yet been elucidated. However, there is a well-documented correlation between the level of IOP and RGC axon loss which has been demonstrated in experimental glaucoma models [13, 14]. As previously stated, while IOP level remains a significant risk factor for glaucoma, not all individuals with ocular hypertension (defined as IOP greater than 21 mmHg) develop glaucoma. In fact, recent findings suggest the majority of individuals with ocular hypertension do not develop glaucoma [1]. Furthermore, some individuals with IOP within the normal range (defined as 10-21 mmHg) develop glaucoma termed "Normal Tension Glaucoma" (NTG). It is estimated that nearly 50% of individuals with open-angle glaucoma have IOP within the normal range and fall under this category [1] while some studies suggest this percentage is even higher [8].

Since IOP alone cannot predict if someone will develop glaucoma, identification of patient-specific biomarkers within the eye could improve the detection and prevention of POAG by catching the disease onset prior to vision loss symptoms. One approach to identify patient-specific biomarkers for POAG is to characterize the mechanical response due to IOP change within the eye, as the geometry and material properties vary slightly in individual eyes. This pilot study sought to validate a method for characterizing the *in vivo* displacement and strain response of the lamina cribrosa (LC) to short-term IOP changes induced by glaucoma medication change.

The level of IOP remains the most relevant risk factor for glaucoma; however, the level of IOP alone cannot definitively predict if an individual will develop glaucoma. Recent research efforts suggest that characterizing the biomechanical response of the eye to IOP change may provide a more effective and patient-tailored approach to assess glaucoma risk [8]. Thus, the goal of the present study was to characterize the short-term biomechanical response of the lamina cribrosa (LC), the primary site of glaucoma damage, to IOP change induced via a change in glaucoma medication, primarily IOP-lowering eye drops. The biomechanical response of the LC to IOP change may be a potential biomarker that could aid in the earlier detection and management of glaucoma.

Much work has been accomplished studying the movement of the anterior lamina cribrosa (ALC) surface and anterior lamina cribrosa depth (ALD) following IOP change. In a recent study, Kim et al. studied the biomechanical response of the LC to IOP-lowering eye drops over the course of one year [15]. They found that in approximately two-thirds of the experimental eyes subjected to IOP-lowering through eye drops, there was a reduction in LC curvature and a greater change in curvature was associated with younger age and higher baseline curvature [15]. This study only assessed the long-term remodeling response to hypotensive drops, which included ALC change and LC curvature change, but did not assess the mechanical strain response. The study by Kim et al. found the ALC surface moves anteriorly after IOP lowering from medication over the course of one year [15]. Conversely, in early experimental monkey eyes, Yang et al. found that the LC migrates posteriorly following IOP elevation with respect to its insertions at the sclera and that this posterior movement is an early step that occurs in excavation [16]. Park et al. investigated ALD in eyes with glaucoma at various stages of progression and found that the posterior movement of the LC is more associated with mild to moderate glaucoma [17]. Additionally, Lee et al. reported a significant reduction in ALC six months following IOP lowering via trabeculectomy [18].

Our group has found that the LC subjected to IOP-lowering can result in decreased or increased ALD 20 minutes after suturelysis, implying the ALC surface can move anteriorly

or posteriorly after IOP lowering [19–21]. ALD change magnitude was not related to IOP change; however, it was significantly associated with having a lower baseline IOP [21]. This suggests ALD change alone is not a sufficient biomarker for glaucoma susceptibility. Other measures of deformation, such as strains, should be analyzed to provide a bigger picture and to provide a normalized measure of deformation due to IOP change.

Previous studies by our group have made progress in characterizing the strain response of the LC and ONH to IOP change. These studies and the current study refer to strains in the Z, R, Θ coordinate system where the Z-direction corresponds to the axial length direction ($Z = 0$ represents the top of the OCT scan and positive Z represents the posterior direction), the R-direction corresponds to the radial direction, and the Θ-direction corresponds to the orientation of cross-sectional OCT images in the R-Z plane with respect to the center of the optic nerve head.

Studies by our group using OCT imaging and DVC to measure *in vivo* strains revealed IOP lowering via post trabeculectomy laser suturelysis resulted in a mean tensile E_{zz} strain in the LC [19, 20], implying IOP-lowering treatments provide strain relief to the LC, allowing it to decompress and expand along its axis relative to the reference state at higher IOP. The study by Lee et al. [18] reported increased LC thickness following IOP lowering six months post trabeculectomy, consistent with our group's findings that the LC expands in the Z-direction following IOP lowering [19, 20]. Using similar methods including OCT imaging, manual segmentation, and a 3D tracking algorithm, Girard et al. found that effective strain relief following IOP lowering via trabeculectomy was greater in eyes with glaucoma compared to healthy eyes and reported a tensile strain of 9.57% in the LC following an IOP decrease of 11.8 ± 8.6 mmHg [22]. In the study by Girard et al., OCT images of the optic nerve head were acquired 21 days prior to trabeculectomy and within 50 days following trabeculectomy, after target IOP was attained [22]. Girard et al. found no association between effective strain magnitude and IOP change [22]. In contrast, Midgett et al. from our group found that a larger maximum principal strain and larger E_{zz} strain in the LC was associated with

increased IOP decrease as well as with increased percent IOP decrease 20 minutes after post trabeculectomy suturelysis, suggesting a nonlinear strain response [19].

When IOP was increased in the eyes of patients wearing tight-fitting swimming goggles, compressive E_{zz} strain was produced [19]. In the suturelysis eyes, the mean E_{rr} strain was compressive [19, 20], suggesting that IOP-lowering treatment also provides strain relief in the radial direction allowing the width of the LC, which is often increased due to high level of IOP and seen in excavation, to contract. Beotra et al. investigated the strain response to acute IOP elevation in normal, ocular hypertensive, and POAG eyes and found that the LC strain response to IOP elevation was greater in healthy eyes than in ocular hypertensive eyes with normal visual fields [23]. Additionally, Beotra et al. found the strain response was greater in healthy eyes than in POAG eyes, however this finding was not statistically significant [23].

Other studies investigated the relationship between the biomechanical response of the LC in relation to glaucoma stage and patient age. In a recent study, Czerpak et al. from our group found LC strains resulting from IOP lowering via suturelysis were more compliant with increased glaucoma damage [20]. Lee et al. found that the magnitude of anterior ALD change after IOP lowering via trabeculectomy was significantly associated with younger age and with greater percent IOP decrease [18].

Previous studies by our group characterized the *in vivo* biomechanical strain response of the LC to IOP lowering via suturelysis after a 20 minute duration [19, 20]. The current study seeks to replicate these experiments in a different population consisting of medication-change patients over a longer duration of one week. Patient volunteers starting glaucoma eye drops were chosen for this study to investigate the biomechanical response to IOP-lowering through a non-invasive means and to investigate this response in a sample population whose glaucoma severity is typically lower than that of glaucoma patients who require invasive treatment. The overall goal of this study was to establish a method for characterizing the short-term *in vivo* biomechanical strain response of the LC to a change in IOP lowering

medication. Recent advances in optical coherence tomography (OCT) and computational algorithms, such as digital volume correlation (DVC), have provided researchers with a safe, noninvasive method to measure displacements and strains in biological tissues *in vivo*. The use of OCT imaging and DVC to measure the *in vivo* biomechanical response of the LC to IOP change were used to achieve this in the present study. To the best of the author's knowledge, this is the first study attempting to measure the short-term (one-week) strain response within the LC using DVC of OCT scans of the ONH before and after IOP change from medication change.

The major aims were to: 1) characterize the *in vivo* ALD change, LC strain response, and strain compliance response to IOP change induced via glaucoma medication change over a period of approximately one week and provide evidence that these measurements are repeatable 2) investigate the relationship of LC strains to IOP change and LC strains to ALD change and 3) investigate the relationship of LC strains and strain compliance to three primary measures of glaucoma damage: RNFL thickness, mean deviation (MD), and visual field index (VFI).

1.3 Biomechanics Overview

The optic nerve head (ONH) at the posterior of the eye is comprised of various tissues including the retina, choroid, sclera, prelaminar neural tissue (PLNT), lamina cribrosa (LC), and the optic nerve whose retinal ganglion cells (RGCs) are found in the retina where they receive a light signal. The RGC axons exit the eye posteriorly in bundles running through the pores of the LC and form the optic nerve which carries the light signal to the brain for interpretation.

As a simple biomechanical model, the eye can be thought of as a fluid-filled, pressurized sphere whose walls are mechanically supported by the sclera. The ONH of the eye is subjected to two major loading conditions. First, the ONH is subjected to stress induced by the

translaminar pressure gradient. This pressure gradient is defined as the difference between IOP and the outside pressure from the retrolaminar tissue. Since IOP generally exceeds the outside pressure, the net stress is caused by IOP; the net compressive stress causes posterior bowing of the ONH (referred to as "excavation" or "cupping") and thinning of the retinal nerve fiber layer (RNFL) [24, 25]. Second, the ONH is subjected to a tensile hoop stress carried by the wall of the eye and transmitted by the PPS. This hoop stress is generated by IOP stress acting normal to the cornea and sclera. The deformation due to hoop stress results in widening the cup feature in glaucoma. Overall, the IOP-generated strain response is complex, involving both the LC and PPS. [24, 26–28]

In general, the translaminar pressure gradient caused by an increased level of IOP is expected to produce greater strains in the LC than in the PPS under the assumption that the LC is less stiff than the PPS. Additionally, the LC is much thinner than the surrounding PPS [24] and is thinner in eyes with glaucoma than in healthy eyes [29]. Furthermore, the LC has a less uniform structure compared to the PPS and its pores allow for stress concentrations making it more susceptible to strain. Therefore, the LC represents a weak point within the wall of the eye. Additionally, regional differences in LC structure affect the overall response to IOP change. The inferior and superior quadrants are especially susceptible to strain since these quadrants are thinner and contain larger pores compared to the nasal and temporal quadrants on average [30]. This leads to greater regional strain associated with increased RGC axon death [20, 30]. The structure of the LC makes it especially susceptible to strains which are linked to detrimental effects such as RGC axonal abnormality as well as decreased blood supply [5]. Deformations within the LC due to elevated levels of IOP in glaucoma are associated with RGC axonal injury, eventually resulting in RGC death and visual field loss; thus, the LC is considered to be the primary site of glaucoma damage [5, 13, 24, 29, 31, 32].

It is important to note that the stiffness of the LC and PPS vary from individual to individual, especially when considering the biomechanical response of the ONH to IOP change since it is mediated by both the LC and PPS. Compliance of the LC for example, is expected

to decrease with age [33]. Furthermore, it is not just the stiffness of the LC that mediates the IOP change response but the combined material properties of the LC and adjacent PPS [24]. A stiffer PPS and more compliant LC would be expected to result in bowing of the LC from increased IOP while a stiffer LC but more compliant PPS, on the other hand, may result in rupture of the LC [24]. If the PPS and LC were both compliant, an increase in IOP may result in elongation of the eye [24]. For the present study, we include measurements of LC strain, while scleral strain measurement methods are still being developed.

Chapter 2

Methods

2.1 Experimental Subjects

Study participants were consenting patients selected from the Johns Hopkins Medical Center's Wilmer Eye Institute's glaucoma division in Baltimore, Maryland. Informed written consent was obtained for all study participants and the study was approved by Johns Hopkins' Institutional Review Board (IRB). All study participants received a standard diagnostic exam for glaucoma prior to participating in the study. Data were originally collected for a total of 35 medication-change eyes from 24 patients, however only data from 23 eyes from 15 patients were included in the study analysis. A total of 12 eyes from 7 patients were excluded from analysis primarily due to poor image quality or poor visibility of the LC, which in some samples was nearly entirely obscured by shadows from the overlying central blood vessels.

All but two eyes included in the study were from patients starting hypotensive eye drops. One study eye was from a patient stopping eye drops and one eye was from another patient starting oral medication to lower IOP. Patient data were collected in two separate sessions: one pre treatment and one post treatment. The mean time between the two sessions was 7.3 $\pm$ 1.4 days.

Data were sampled from eyes with varying glaucoma severity, however, the patient de-

mographic for this study was biased towards patients with mild glaucoma damage, defined as mean deviation (MD) greater (better) than -6 dB. The sample population included eyes from males and females of African American, Asian, and Caucasian descent and was biased towards patients of female sex and Caucasian descent. The sample population had an age range of 30 to 80 years, a mean age of 62.1 $\pm$ 12.4 years, and a median age of 64 years (Table 2.1). A detailed summary of specimen data for each eye (including patient demographics, IOP change mode, and MD) may be found in the appendix (Table A.2).

The subjects were divided into two groups. Group 1 consisted of 17 eyes from 12 patients who received IOP-lowering medication and underwent an IOP change in magnitude of at least 4 mmHg after one week. This threshold was chosen based on prior work by our group which demonstrated that the method used in the present study can measure significant strains resulting from IOP changes as small as 2 mmHg [19]. Group 2 consisted of 6 eyes from 5 patients who received IOP-lowering medication and did not undergo a significant IOP change (defined as a change of 0-1 mmHg to allow for error from the tonometer) after the treatment period. No eyes had an IOP change magnitude between 1 mmHg and 4 mmHg.

Both experimental study groups consisted of eyes undergoing a change in glaucoma medication. These changes included starting newly prescribed hypotensive eye drops, stopping eye drops, or starting oral medication to lower IOP. Eyes starting a new glaucoma medication were expected to undergo a decrease in IOP within one week, and the mean time after the treatment change was 7.3 days $\pm$ 1.4 days. Strains resulting from IOP decrease were representative of strain change compared to the reference state. The eyes of patients stopping glaucoma medication were expected to undergo an increase in IOP after one week, representative of increased strain relative to the reference state.

Table 2.1: Glaucoma medication-change patient demographics for entire medication-change group and its two subgroups based on IOP change: Group 1 and Group 2. Group 1 consisted of medication-change eyes with IOP change of at least 4 mmHg. Group 2 consisted of medication-change eyes with IOP change of 0-1 mmHg and functioned as a "pseudo control" group. There were no eyes with an IOP change between 1 and 4 mmHg. *Sample Size is reported as (x, y) where x is the number of eyes from y patients.

	All (Group 1 & Group 2)	**Group 1**	**Group 2**
Sample Size*	23, 15	17, 12	6, 5
Age (years)	62.1 ± 12.4	62.2 ± 13.7	61.8 ± 9.0
Sex	15 F, 8 M	11 F, 6 M	4 F, 2 M
Medication-Change Period (days)	7.3 ± 1.4	7.3 ± 1.4	7.5 ± 1.2
Baseline IOP (mmHg)	18.3 ± 6.6	20.3 ± 5.8	12.5 ± 5.2
IOP Change (mmHg)	-4.3 ± 2.8	-5.8 ± 1.5	-0.3 ± 0.8
MD (dB)	-6.0 ± 5.7	-6.6 ± 5.8	-4.3 ± 5.8
VFI	0.86 ± 0.13	0.85 ± 0.13	0.90 ± 0.14
Average RNFL (μm)	66.6 ± 8.0	65.2 ± 7.3	70.7 ± 9.1

2.2 Tonometry

Intraocular pressure (IOP) was measured in each eye using a rebound tonometer (iCare TA01i, iCare Finland Oy, Espoo, Finland). The iCare tonometer was used to measure IOP in this study due to its high accuracy and high reproducibility comparable to that of Goldmann applanation tonometry. The iCare tonometer has a reported accuracy of ± 1.2 mmHg (20 mmHg) and ± 2.2 mmHg (> 20 mmHg) for a 95% tolerance interval relative to manometry and repeatability (coefficient of variation) less than 8. In addition to providing accurate and consistent measurements, the iCare tonometer was selected for operational convenience as it does not require a local anesthetic prior to use nor specialized training to use [34].

IOP for each study eye was measured prior to each imaging session using the iCare tonometer. Baseline or pre-treatment IOP and post-treatment IOP were each recorded as the mean of six consecutive measurements per eye. Repeated measurements were taken to

determine the average IOP in each eye until the tonometer screen displayed a low or no variability mean IOP reading. An average IOP reading with low variability indicated the standard deviation of the six consecutive measurements was higher than normal but was considered acceptable, as low variability is unlikely to impact the result [34]. If the initial mean IOP reading indicated high variability, the average of two no or low variability means was recorded as the final IOP measurement. For each eye, IOP values obtained by the iCare tonometer were compared to the Goldmann applanation values measured immediately before by a technician or ophthalmologist.

All IOP measurements were taken with patients sitting in an upright position and without use of a local anesthetic. Patients were directed to look forward such that the chin was parallel to the ground. Measurements were taken with the rebound tonometer probe positioned perpendicularly to the surface of the central cornea with the tip of the probe approximately 4 to 8 mm away.

2.3 Ocular Biometry

In order to prepare for optical coherence tomography imaging, the average axial length and corneal curvature of each eye were measured using an IOL Master (Carl Zeiss Meditec, Inc., Dublin, CA, USA) (Fig. 2.1), an ocular biometry instrument based on partial coherence interferometry (PCI), a non-contact method routinely used in ophthalmology that offers high resolution and high reproducibility [35]. Axial length measurement was taken as the average of five subsequent measurements. In order to calibrate the OCT instrument's optical magnification for each eye, corneal curvature was taken as an average of the maximum and minimum measurements at baseline IOP and at IOP post-treatment.

Figure 2.1: The IOL Master, a standard instrument widely used in ophthalmic clinics, was used to measure the axial length and curvature of each eye

2.4 Optical Coherence Tomography (OCT)

Optical coherence tomography (OCT) is an imaging modality extensively used in ophthalmology to image the layers of the retina and visualize structures of the optic nerve head which may be used for glaucoma diagnostic testing, among other clinical applications. The principle behind OCT is analogous to that of ultrasound imaging, except OCT utilizes light waves instead of sound waves.

In OCT imaging, light travels to the tissue sample, is backscattered by the retinal layers and other soft tissue layers of the ONH, then interferes with a light ray sent to a mirror with a known time delay for reference [36]. Using time delay information, the depth profile of the reflected light relative to echo delay can be reconstructed. This occurs at a single point and is known as an amplitude scan or A-scan. Scanning a sample laterally at multiple points results in a grayscale cross-sectional image, known as a B-scan (brightness scan),

where the grayscale value at each point represents the brightness amplitude of the reflected light [36, 37]. Consecutive sectional OCT scans may be stacked to form a 3D image volume. The present study acquired B-scans spaced at equal intervals circumferentially around the optic nerve head. This resulted in 2D cross-sectional images in which the height of the scan represented the axial direction, and the length of the scan represented the radial direction. These are known as radial B-scans.

OCT offers a noninvasive and clinically available method to image the layers of the retina and optic nerve head of glaucoma patients *in vivo*. OCT uses a low-power laser as its light source, making it a safe imaging method. Additionally, OCT is fast enough to acquire images in real time. OCT instrumentation primarily consists in two configurations: spectral domain and time domain. Spectral domain OCT (SD-OCT) was used in the present study due to its higher speed and higher resolution compared to time domain OCT (TD-OCT), as well as its increasing use in biomedical applications [38]. Additionally, studies have shown that SD-OCT provides better measurement repeatability compared to TD-OCT [39].

The optic nerve head (ONH) of each study eye was imaged using a Spectralis instrument (Heidelberg Engineering, Heidelberg, Germany) (Fig. 2.2) at the baseline IOP and at IOP post treatment. Patients were imaged in an seated position with the chin rest adjusted so that the patient's chin was parallel to the ground. After turning off the lights, patients were directed to look forward, focusing on a target light, and blink several times before image acquisition. Images were acquired with the OCT instrument set to high resolution and auto-brightness mode. To optimize image quality and visibility of the LC, the OCT was adjusted such that the brightness of the visible tissue was as high as possible, and the tissue cross section was positioned such that it occupied the lower two-thirds of the window. During each imaging session, three consecutive image volumes were taken for each eye approximately 30 seconds apart. After the first volume was acquired, the subsequent volumes were automatically oriented by the Heidelberg software registration.

Each image volume consisted of 24 radial B-scans (optical cross-sections) centered about

Figure 2.2: The Heidelberg Spectralis was used at each imaging session to acquire radial OCT image volumes consisting of 24 slices per volume

the ONH (Fig. 2.3A). Circumferential scans were taken in 7.5° clockwise steps with the first scan oriented perpendicular to the axis connecting the center of the Bruch's membrane opening and the fovea. The resolution of each scan was 768 × 495 in the (R, Z) plane and had a resolution in the Z-direction (anterior-posterior) of 3.87 μm/pixel. Resolution in the R (radial) direction ranged from 5.95 ± 0.29 (5.66 – 6.24) μm/pixel. Resolution in the R-direction varied among each eye due to the optical magnification used to adjust for patient-specific corneal curvature of each eye. The R-scaling factor for each eye determined by the Heidelberg software was recorded for DVC analysis. [19]

2.5 Image Processing and Segmentation

Radial OCT scans were pre-processed using MATLAB (R2019a, Mathworks, Natick, MA, US). The 24 de-identified OCT scans for each volume were cropped to render 768 x 495-pixel cross-sectional images of the retina. Images were then converted into 8-bit intensity-valued

pixels (Fig. 2.3B). Each image was trimmed of 13 pixels on the left and right edges to reduce errors associated with DVC calculation along image borders. Additionally, 35 pixels were cropped from the bottom (posterior) image border to remove overlaid scale bars, rendering 642 x 460-pixel images. Furthermore, each scan was vertically cropped about the horizontal midpoint such that R = 0 corresponded to the center of the ONH in each image and Z = 0 corresponded to the top (anterior) border of the image. The circumferential direction, or Θ-direction, was oriented such that $\Theta = 0^\circ$ corresponded to the inferior-superior cross-section. This created a set of 371 x 360 x 48 images per image volume spaced 7.5° apart circumferentially about the ONH. [19]

All image volumes were filtered and contrast-enhanced in ImageJ Fiji [40] (Fig. 2.3C), using the software's contrast-limited adaptive histogram equalization (CLAHE) algorithm, a modified version of adaptive histogram equalization (AHE) designed to minimize noise amplification. It has been demonstrated that CLAHE contrast enhancement can improve DVC correlation [19, 41]. Within CLAHE, the block size was set to 14, the histogram bins were set to 256, the maximum slope was set to 3.5, and the mask was set to "None" type. In addition to CLAHE, a gamma filter with a correction value of 1.75 was used to preserve tissue speckle patterns within each image to prevent filtering out fine tissue details as noise. Preserving the unique speckle pattern within each image of the ONH tissue was crucial for optimizing DVC correlation.

In preparation for DVC, the filtered image volume acquired at baseline IOP with the greatest focus and least noise was selected for each eye. Several soft tissue layers of the ONH in each scan were segmented by hand in ImageJ Fiji (V.H.) and verified by an ophthalmologist (H.A.Q.) (Fig. 2.4). For each scan, the Bruch's membrane opening (BMO), the posterior border of Bruch's membrane, the choroid-sclera interface, and the anterior LC border were segmented, and each structure's pixel coordinates (R, Z, Θ) were saved for DVC analysis (Fig. 2.4A). The BMO was marked twice per scan and a horizontal line was drawn between the two points to define the BMO width. The Bruch's membrane, choroid-sclera interface,

and ALC border were marked without a set number of points such that the points were spaced approximately every 15-25 pixels. The ALC border was only marked within the BMO width. Anterior LC depth (ALD) was defined as the vertical distance between the BMO width and the ALC border. The left and right Bruch's membranes and the left and right choroid sclera interfaces were segmented in order to obtain DVC-calculated strains in the retina, choroid and sclera, which may be used for future work. [19]

After importing the pixel coordinates of each hand-segmented boundary, the ALC was segmented from the posterior lamina cribrosa (PLC) by drawing a border 250 µm posterior to the ALC in MATLAB (Fig. 2.4B). The ALC region was defined with a thickness of 250 µm based on the average histological thickness for the human ALC and was additionally based upon the previous method employed by our group for estimating *in vivo* strains in the human LC [19, 42].

2.6 DVC Analysis and Strain Calculations

Digital volume correlation (DVC) is a 3D extension of digital image correlation (DIC), which calculates full displacement and strain fields, and is based on finite element analysis principles. DVC is becoming an increasingly popular method within the biomechanics field for analyzing *in vivo* tissue deformation [43]. DVC is suitable for correlating images with random, high-contrast speckle or intensity patterns [44, 45]. In the present study, the natural speckle patterns of the LC were visible in OCT scans. Our group and others have demonstrated DVC is a valid method for quantifying strains in OCT scans of the ONH [19, 20, 46–48].

DIC estimates displacements from the reference image to the deformed image by correlating groups of pixels in specified correlation windows, also known as subsets. The correlation window contains a unique "signature" from the reference image which is composed of a central pixel surrounded by neighboring pixels [45]. The size of the correlation window may

be specified by the user. First, the algorithm searches for the signature in the deformed image using the specified correlation window. Various locations in the deformed image are checked for possible matches. The possible matches are given a score based on a correlation function which is usually the sum of squared differences of the pixel values. The smallest score (smallest difference) is chosen as the best match. Displacement fields are calculated as the average of pixel displacements contained in the window. From the displacement fields, the resulting strain fields may be derived. [19, 20, 45]

In the current study, a fast-iterative DVC algorithm was used to calculate IOP change-related strain fields in the LC from medication change. This algorithm, used in previous work by our group, allowed for iterative refinement of the window size and spacing to optimize speed and accuracy [1, 48]. The fast-iterative DVC algorithm developed by the Bar-Kochba group [43] was used to compute displacement fields and the corresponding strain fields as a result of IOP change from glaucoma medication change. Prior to performing DVC in MATLAB, the radial scaling factor (μm/pixel) and whether the eye was a left eye or right eye were specified. The DVC correlation coefficient was held constant at 0.055 and the best reference image, second best reference image, and best post-treatment image were designated within the code. The (R, Z, Θ) pixel coordinates for each hand-segmented ONH region were imported into the code to define the regional boundaries for DVC post-processing. This allowed for obtaining the average strain within the ALC, retina, choroid, and sclera.

Displacements in the R, Z, and Θ direction were calculated by applying DVC to the undeformed reference image (image taken at baseline IOP) and the deformed image (image taken at post-treatment IOP). The pixel displacements were later converted to μm displacements using the recorded scaling factors. Displacement gradients with respect to R and Z for locally defined pixel neighborhoods within the R-Z plane were determined by local displacement fitting [19]. Displacement gradients with respect to the Θ-direction were determined by 4th order polynomial fitting for displacements at every in-plane (R, Z) pixel for all image volume slices [19]. To ensure boundary continuity, polynomial fitting for displacements was

repeated twice for image slices oriented at $\Theta = 0$ and $\Theta = 2\pi$ [19].

From the displacements, the strain tensor was calculated in cylindrical coordinates using the standard Green-Lagrange strain equations (Eq. 2.1 - 2.6).

$$E_{rr} = \frac{\delta U_r}{\delta r} + \frac{1}{2}\left[\left(\frac{\delta U_r}{\delta r}\right)^2 + \left(\frac{\delta U_\theta}{\delta r}\right)^2 + \left(\frac{\delta U_z}{\delta r}\right)^2\right] \tag{2.1}$$

$$E_{zz} = \frac{\delta U_z}{\delta z} + \frac{1}{2}\left[\left(\frac{\delta U_r}{\delta z}\right)^2 + \left(\frac{\delta U_\theta}{\delta z}\right)^2 + \left(\frac{\delta U_z}{\delta z}\right)^2\right] \tag{2.2}$$

$$E_{rz} = \frac{1}{2}\left[\frac{\delta U_r}{\delta z} + \frac{\delta U_z}{\delta r} + \frac{\delta U_z}{\delta r}\frac{\delta U_z}{\delta z} + \frac{\delta U_\theta}{\delta r}\frac{\delta U_\theta}{\delta z} + \frac{\delta U_z}{\delta r}\frac{\delta U_z}{\delta z}\right] \tag{2.3}$$

$$E_{\theta\theta} = \frac{U_r}{r} + \frac{1}{r}\frac{\delta U_\theta}{\delta \theta} + \frac{1}{2}\left[\frac{1}{r^2}\left(\frac{\delta U_z}{\delta \theta}\right)^2 + \left(\frac{1}{r}\frac{\delta U_r}{\delta \theta} - \frac{U_\theta}{r}\right)^2 + \left(\frac{1}{r}\frac{\delta U_\theta}{\delta \theta} + \frac{U_r}{r}\right)^2\right] \tag{2.4}$$

$$E_{\theta r} = \frac{1}{2}\left[\frac{\delta U_\theta}{\delta r} + \frac{1}{r}\left(\frac{\delta U_r}{\delta \theta} + \frac{\delta U_r}{\delta \theta}\frac{\delta U_r}{\delta r} + \frac{\delta U_z}{\delta \theta}\frac{\delta U_z}{\delta r} + \frac{\delta U_\theta}{\delta \theta}\frac{\delta U_\theta}{\delta r} + U_r\frac{\delta U_\theta}{\delta r} - U_\theta\frac{\delta U_r}{\delta r} - U_\theta\right)\right] \tag{2.5}$$

$$E_{\theta z} = \frac{1}{2}\left[\frac{\delta U_\theta}{\delta z} + \frac{1}{r}\left(\frac{\delta U_z}{\delta \theta} + \frac{\delta U_z}{\delta \theta}\frac{\delta U_z}{\delta z} + \frac{\delta U_r}{\delta \theta}\frac{\delta U_r}{\delta z} + \frac{\delta U_\theta}{\delta \theta}\frac{\delta U_\theta}{\delta z} + U_r\frac{\delta U_\theta}{\delta z} - U_\theta\frac{\delta U_r}{\delta z}\right)\right] \tag{2.6}$$

From the 2D strain tensor (E_{rr}, E_{zz}, E_{rz}), maximum principal strain, E_{max}, and maximum shear strain, Γ_{max}, were determined for strains contained in the R-Z plane, the plane imaged by the OCT radial scans (Eq. 2.7 - 2.8). Maximum principal strains were not calculated using the 3D strain tensor due to displacement resolution in the Θ-direction growing poorer as radial distance increased [19].

$$E_{max} = \frac{E_{rr} + E_{zz}}{2} + \sqrt{\left(\frac{E_{rr} - E_{zz}}{2}\right)^2 + E_{rz}^2} \tag{2.7}$$

$$\Gamma_{max} = \sqrt{\left(\frac{E_{rr} - E_{zz}}{2}\right)^2 + E_{rz}^2} \tag{2.8}$$

The compliance of each strain response was determined by dividing each strain by the corresponding IOP change magnitude for that eye. Similarly, the compliance of the ALD change response from IOP change was calculated by dividing the ALD change by the cor-

responding IOP change magnitude for that eye. The expressions used to obtain each strain compliance are listed in the Appendix under Section A.3.

Strain correlation error was determined by taking the difference between the applied strain and the observed strain determined by DVC. The observed strain was calculated by duplicating the reference image volume (image at baseline IOP) and warping it with a known stretch value, then calculating the resulting displacement and strain fields using DVC. Based on previous methods by our group [19], the warped reference image was created by applying a rigid body translation of 10 µm in the Z-direction followed by a uniform 2% tensile strain in the R-direction and 2% compressive strain in the Z-direction. To account for error due to eye movement and blood vessel pulsation, strain baseline error was calculated by taking the difference between strain calculated in DVC for duplicate image volumes (two image volumes taken 30 seconds apart) for the same eye at baseline IOP.

The DVC results were post-processed within the MATLAB code to minimize strain error resulting from displacement correlation error. A DVC correlation filter was used to remove areas with poor displacement correlation, reduce displacement errors along image borders, and remove displacements with average absolute displacement error greater than 0.25 pixel by using threshold and subset size settings previously determined by our group [19]. Additionally, the filter was designed to minimize calculating displacements outside of tissue boundaries.

Regions containing correlation coefficients less than the threshold of 0.055 were considered to have poor contrast that may increase correlation error and were removed by the DVC correlation filter. To reduce displacement correlation errors along boundaries containing the tissue sample, displacement calculations were excluded if they fell within 25 pixels of the bottom (posterior) image border or within 32 pixels from the left or right image border [19]. DVC often results in higher correlation errors along boundaries due to discontinuities; excluding the boundaries from DVC analysis is a common practice [49]. Field discontinuities within the target analysis area can further increase correlation error [50]. Thus, displace-

ments fields and discontinuities in the R-Z plane were smoothed using a 2D Gaussian filter developed by our group [19]. Out-of-plane displacements corresponding to the circumferential or Θ-direction were smoothed using a 1D Gaussian filter for each image slice at each in-plane (R, Z) pixel [19]. The Gaussian smoothing filters were designed to reduce spikes in the displacement field while maintaining the average gradient [19]. Finally, in-plane displacement outliers were filtered by removing U_r and U_z displacements exceeding 5 μm or exceeding the average displacement within a locally defined neighborhood by 10 μm [19].

2.7 Statistical Analysis

All data reported in the current study were represented as mean ± standard deviation. The study included 23 eyes from 15 patients for the entire medication-change group (Group 1 and Group 2), 17 eyes from 12 patients for Group 1, and 6 eyes from 5 patients for Group 2, unless otherwise specified. For all statistical analyses, a p-value of 0.05 or less was considered significant and a p-value between 0.05 and 0.10 was considered borderline significant.

To determine whether DVC-measured strains after IOP change were significantly different from zero, mean strains were compared to zero using a paired t-test. Paired-sample t-tests were also used to determine if mean strains exceeded their corresponding mean baseline error and mean correlation error. Linear regression analysis was used to test relationships between strains, IOP change, IOP percent change, ALD change, damage, and age. For all statistical tests conducted in the current study, normal distribution of the data was assumed. The statistical analyses in the current study did not account for inter-eye correlation effects.

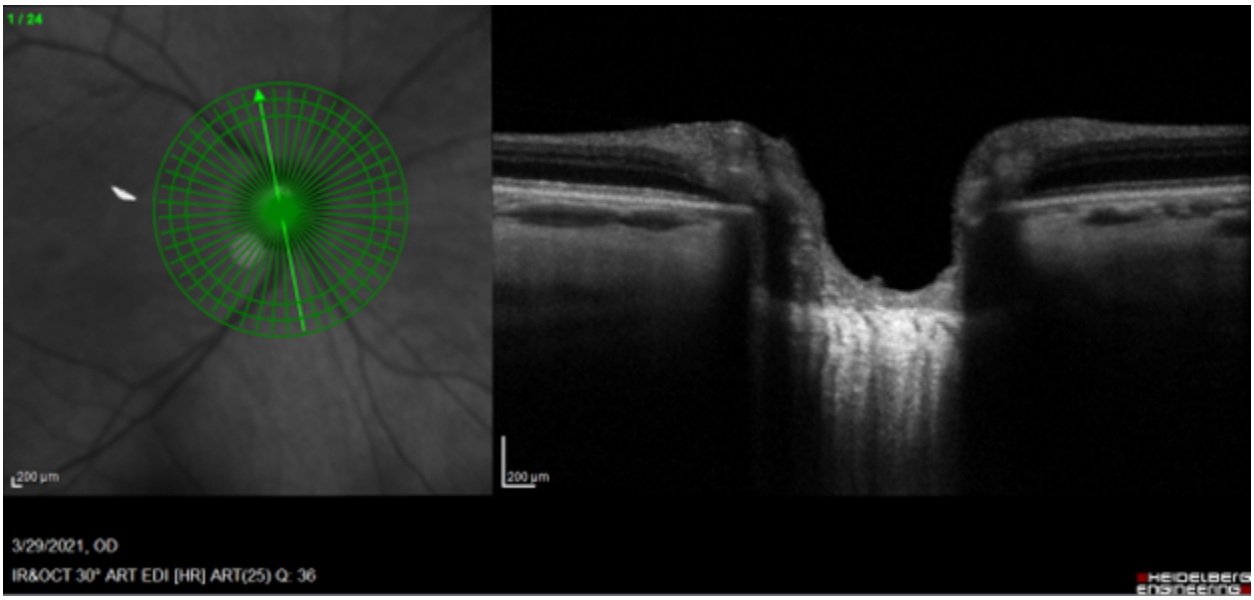

(A)

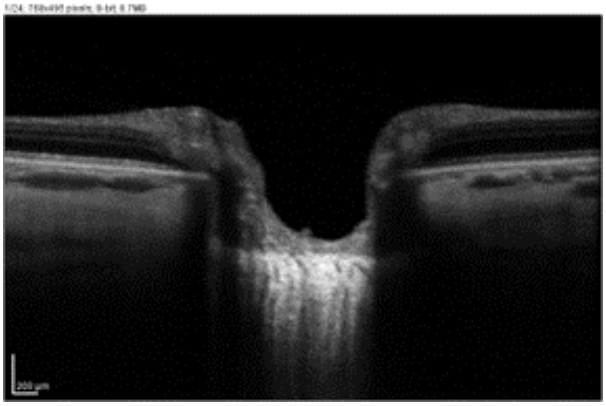

(B)

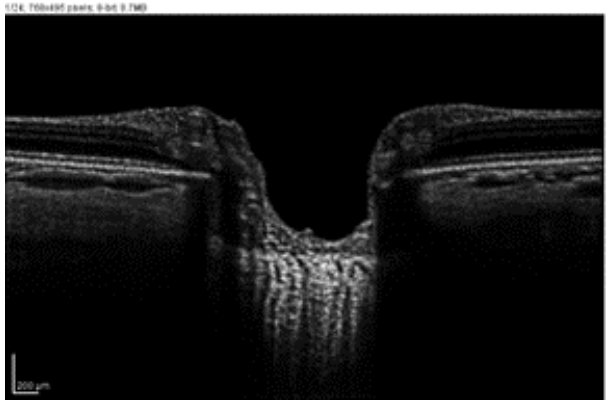

(C)

Figure 2.3: Radial OCT scans of the ONH were acquired using the Heidelberg OCT. Each OCT image volume consisted of 24 evenly spaced slices. **A)** Original scan and orientation map. **B)** The original OCT image after cropping in Matlab. **C)** Image processed with CLAHE and a gamma filter to enhance contrast of the speckle pattern to optimize DVC correlation.

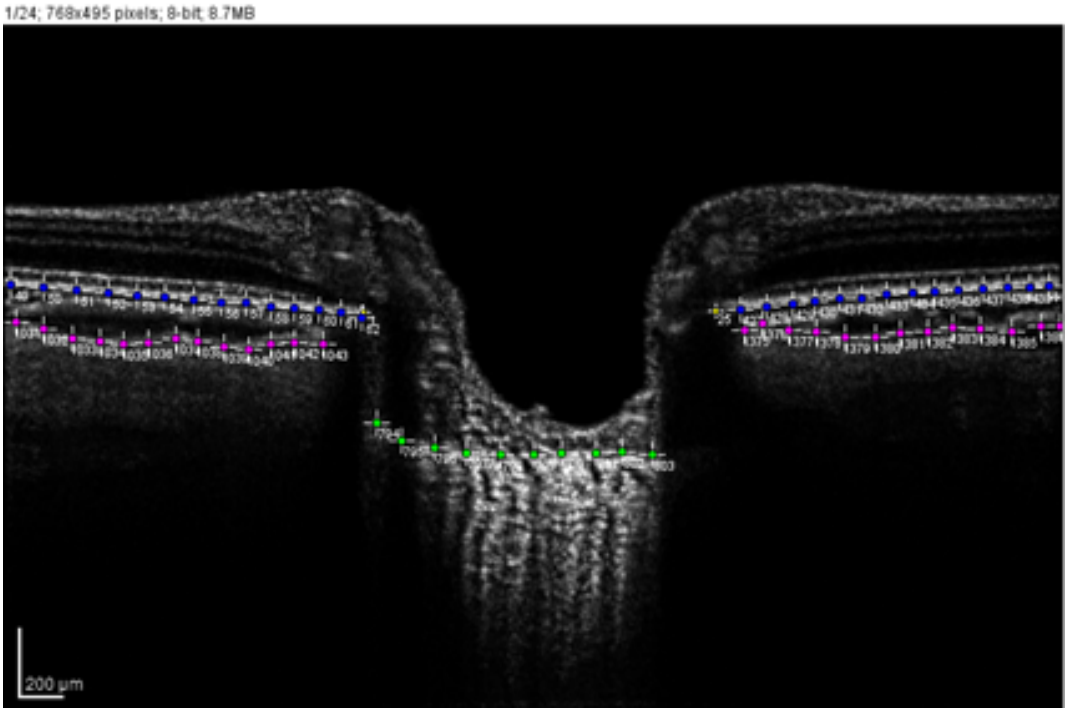

(A)

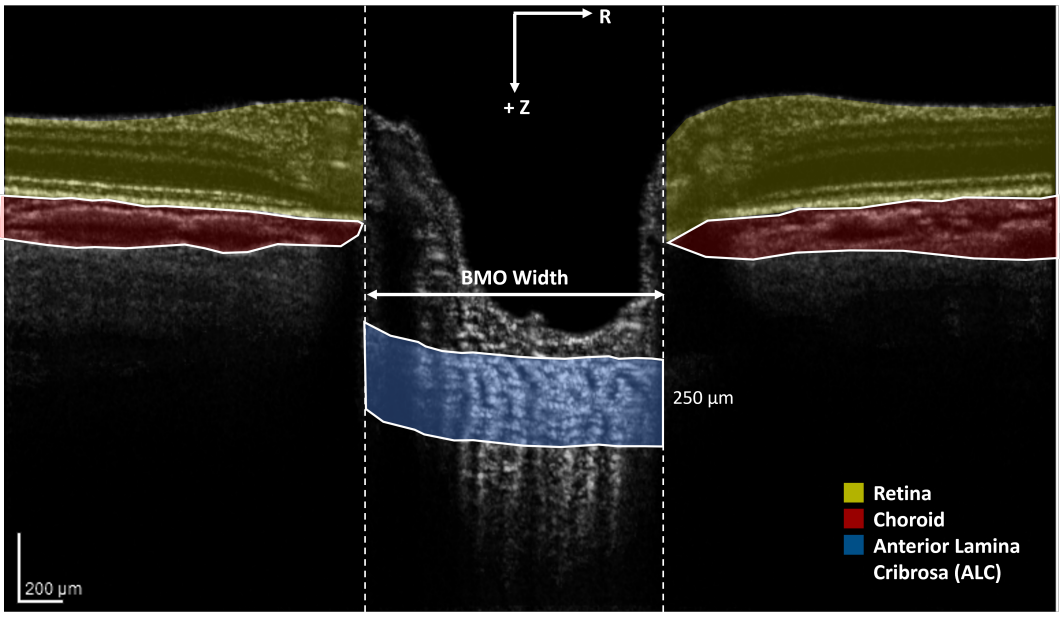

(B)

Figure 2.4: The optic nerve head in each of the 24 slices in every OCT volume was segmented by hand in ImageJ to define the boundaries of the ALC, retina, choroid, and sclera. The posterior border of the ALC was segmented automatically in MATLAB by drawing a border 250 μm below the anterior border of the ALC. The pixel coordinates were imported into MATLAB for DVC post-processing analysis. **A)** Hand-segmented image in ImageJ Fiji. Green = ALC border, Yellow = Bruch's Membrane Opening, Blue = posterior border of Bruch's Membrane, and Magenta = choroid/sclera interface. **B)** Representation of final segmented image in the R-Z plane. Z = 0 corresponds to the top of the image and R = 0 corresponds to the center of the image.

Chapter 3

Results

3.1 IOP Change as a Result of Glaucoma Medication Change

After the treatment period, IOP decreased modestly, and the mean IOP change was -4.4 ± 2.8 mmHg for the entire group (23 eyes from 15 patients) (Fig. 3.1). The mean IOP change for Group 1 was -5.8 ± 1.5 mmHg (p = 4.166E-11, paired t-test), while the mean IOP change for Group 2 was -0.3 ± 0.8 mmHg (p = 0.363, paired t-test). The entire medication-change group (Group 1 and Group 2) had a percent IOP lowering of 22.6% ± 14.5%, Group 1 had an IOP percent lowering of 29.6% ± 8.2%, and Group 2 had an IOP percent lowering of 2.7 % ± 8.1%.

3.2 Anterior LC Depth (ALD) Change

The mean ALD displacement for all experimental groups was positive (movement out of the eye) after IOP lowering (Fig. 3.2), equaling 2.32 ± 3.40 μm (p = 0.004 for difference from no mean change, paired t-test). However, as suggested by the high variability denoted by the standard deviation, the ALC border moved posteriorly in some cases and anteriorly in

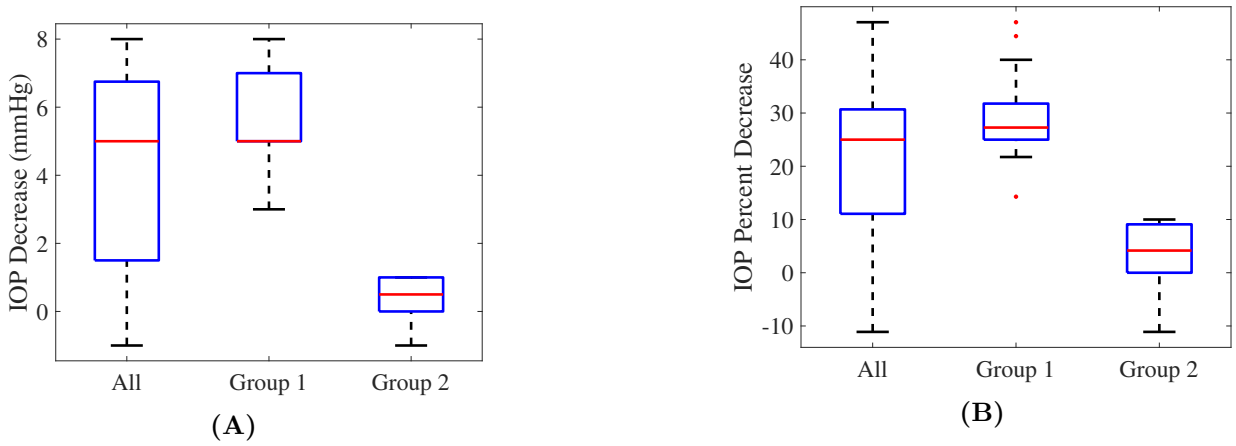

Figure 3.1: After an average of one week from starting glaucoma medication (hypotensive eye drops), IOP decreased in some but not all medication-change eyes. The entire medication-change group was subdivided into two groups based on IOP decrease magnitude. Group 1 contained eyes with an IOP change of at least 4 mmHg while Group 2 contained eyes whose IOP did not change after the treatment period (defined as an IOP change of 0-1 mmHg). No eyes underwent an IOP change between 1 and 4 mmHg. **A)** IOP decrease magnitude. **B)** IOP percent decrease.

others. For Group 1, mean ALD displacement was posterior, 2.61 $\pm$ 3.73 μm (p = 0.011) and for Group 2, the mean displacement was 1.50 $\pm$ 2.27 μm (0.167). The results for ALD change are reported in Table 3.1.

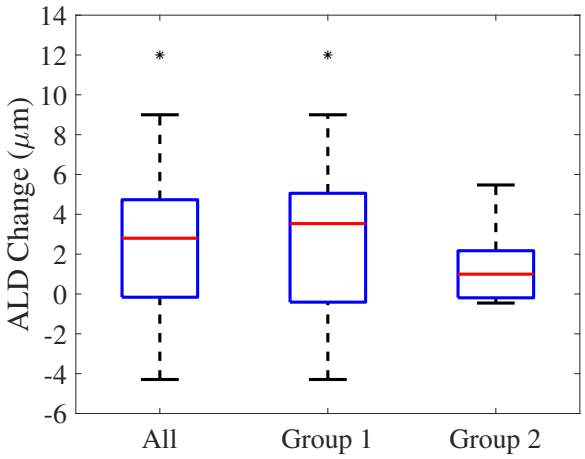

Figure 3.2: ALD Change (μm) after IOP change induced via glaucoma medication change was calculated using DVC. A positive ALD change represents posterior displacement of the ALC border while a negative ALD change represents anterior displacement. An asterisk indicates the group mean was significantly different from zero (p-value less than or equal to 0.05). The median ALD change was positive for all groups and was significant for the entire medication-change group and Group 1, suggesting on average the ALC border moved posteriorly after IOP change over the course of one week.

3.3 LC Strains as a Result of Medication Change

Paired t-tests were conducted to test whether each mean strain resulting from IOP change was significantly different from zero. The distribution of the LC strain response to IOP change across all medication-change eyes was plotted in MATLAB for visualization (Fig. 3.3). and tabulated in Table 3.1. For the entire medication-change group, mean IOP decrease (-4.4 ± 2.8 mmHg) induced by initiating glaucoma medication resulted in mean E_{zz} strain that was tensile, 0.8% ± 1.0% (p = 0.0004, paired t-test) that exceeded baseline error (p = 0.00314). This indicated that, on average, the LC expanded in the Z- or axial direction (anterior-posterior) relative to the reference state. The maximum principal strain, E_{max}, was 1.6% ± 1.1% and the maximum shear strain, Γ_{max}, was 1.3% ± 0.7% (p = 5.03E-7 and p = 4.24E-8, respectively; paired t-test). The IOP decrease was associated with a compressive E_{rr} strain of -0.2% ± 0.6% that was not statistically significant (p = 0.125).

For Group 1, mean IOP decrease of -5.8 ± 1.5 mmHg resulted in tensile mean E_{zz} strain of 1.0% ± 1.1%; p = 0.003, paired t-test) and compressive mean E_{rr} (E_{rr} = -0.3% ± 0.5%; p = 0.012). Group 1 also had significant E_{max} (1.7% ± 1.0%; p = 5.35E-6) and Γ_{max} (1.4% ± 0.7%; p = 4.33E-9). E_{zz} exceeded baseline error (p = 0.00532) and E_{rr} each significantly exceeded both baseline and correlation error (p = 0.0225 and p = 0.0309, respectively).

For Group 2, there were only borderline significant strains in E_{max}, Γ_{max}, and E_{zz} (p = 0.053, p = 0.041, and p = 0.054, respectively; paired t-test). The mean E_{zz} for Group 2 was 0.3% ± 0.3%, was borderline greater than baseline error (p = 7.52E-2) and was about three times smaller than the mean E_{zz} for Group 1.

3.4 Regional LC Strains, ALD Change, and RNFL

For the entire medication-change group, there were no significant differences between the central and peripheral LC in mean E_{zz} or mean E_{max}. Furthermore, there were no differences in mean E_{zz}, mean E_{max}, or mean ALD change by quadrant of the LC (ANOVA).

Table 3.1: Strains and ALD change in the LC following IOP change were quantified using DVC for the entire medication-change group, Group 1, and Group 2. IOP lowering from starting glaucoma eye drops resulted in a positive (tensile) E_{zz} strain for all groups, indicating the LC expanded along the Z-direction (axial direction or anterior-posterior direction). However, the magnitude of E_{zz} for Group 2 (eyes that did not undergo significant IOP change), was approximately three times smaller than that of Group 1. E_{rr} was negative (compressive) and significant for Group 1, demonstrating the LC contracts in the radial direction following IOP lowering from eye drops. On average, ALD change was positive and significant for Group 1 and the entire medication-change group, indicating that the LC surface migrated posteriorly.

	All (Group 1 & Group 2)	**p-value**	**Group 1**	**p-value**	**Group 2**	**p-value**
$\boldsymbol{E_{zz}}$	0.008 ± 0.010	0.001	0.010 ± 0.011	0.003	0.003 ± 0.003	0.054
$\boldsymbol{E_{rr}}$	-0.002 ± 0.006	0.125	-0.003 ± 0.005	0.012	0.001 ± 0.009	0.762
$\boldsymbol{E_{\theta\theta}}$	-0.001 ± 0.008	0.516	-0.001 ± 0.009	0.699	-0.002 ± 0.009	0.762
$\boldsymbol{E_{r\theta}}$	-0.001 ± 0.012	0.560	0.002 ± 0.008	0.354	-0.011 ± 0.017	0.196
$\boldsymbol{E_{\theta z}}$	-0.001 ± 0.005	0.553	-0.001 ± 0.005	0.323	0.001 ± 0.006	0.653
$\boldsymbol{E_{rz}}$	-0.001 ± 0.005	0.637	0.000 ± 0.006	0.770	-0.001 ± 0.004	0.626
$\boldsymbol{E_{max}}$	0.016 ± 0.011	0.000	0.017 ± 0.010	0.000	0.013 ± 0.012	0.053
$\boldsymbol{\Gamma_{max}}$	0.013 ± 0.007	0.000	0.014 ± 0.007	0.000	0.011 ± 0.009	0.041
ΔALD (μm)	2.318 ± 3.400	0.004	2.607 ± 3.734	0.011	1.498 ± 2.269	0.167

The average RNFL thickness was 66.61 ± 7.99 μm for the entire medication-change group, and, as expected from the normal distribution of RNFL, the RNFL thickness means varied significantly by LC quadrant (p = 3.27E-12). RNFL was 76.74 ± 11.35 μm in the inferior quadrant, 80.09 ± 15.38 μm in the superior quadrant, 61.13 ± 12.09 μm in the nasal quadrant, and 48.74 ± 14.13 μm in the temporal quadrant. RNFL thickness was greater in the inferior quadrant than in the nasal and temporal quadrants (p = 1.1E-3 and p = 0.0000, respectively). Additionally, RNFL thickness was greater in the superior quadrant than in the nasal and temporal quadrants (p = 1E-4 and p = 0.0000, respectively). Finally,

RNFL thickness was greater in the nasal quadrant compared to the temporal quadrant (p = 1.36E-2).

3.5 LC Strains, ALD Change, and IOP Change

Linear regression was used to assess whether IOP decrease magnitude was significantly related to strain magnitude. For the entire medication-change group, there was a borderline negative association between E_{rr} and IOP decrease ($R^2 = 0.156$, $p = 0.062$), where E_{rr} became more negative (compressive) with increased IOP decrease. Additionally, there was a borderline positive association between Γ_{max} and IOP decrease ($R^2 = 0.125$, $p = 0.098$), where Γ_{max} increased in magnitude with increased IOP decrease. There were no significant associations between the other unique components of the strain tensor—E_{zz}, E_{rz}, $E_{\theta z}$, and $E_{r\theta}$—with IOP decrease. Furthermore, neither E_{max} nor ALD change was associated with IOP decrease.

In Group 1, greater Γ_{max} was associated with a greater magnitude of IOP decrease ($R^2 = 0.313$ $p = 0.019$, linear regression). E_{max} was borderline larger for larger IOP decrease ($R^2 = 0.192$, $p = 0.079$). There was no association between E_{rr} and IOP decrease for Group 1. Furthermore, there were no associations between the other strain components and IOP decrease, nor was there an association between ALD change and IOP decrease.

Strains and ALD change magnitude were also compared to percent IOP decrease. For the entire medication-change group, greater Γ_{max} was associated with greater IOP percent decrease ($R^2 = 0.222$, $p = 0.023$, linear regression) and greater E_{max} was borderline associated with greater IOP percent decrease ($R^2 = 0.125$, $p = 0.099$). A more negative (compressive) E_{rr} correlated with greater IOP percent decrease ($R^2 = 0.234$, $p = 0.019$), while E_{zz}, $E_{\theta\theta}$, E_{rz}, $E_{\theta z}$, $E_{r\theta}$, and ALD change were not significantly associated with IOP percent decrease. In Group 1, E_{max} increased in magnitude more with greater percent IOP decrease (Fig. 3.5B) than with IOP decrease magnitude (Fig. 3.5A). The same relationship was observed

even more strikingly for Γ_{max}, in which Γ_{max} increased in magnitude more with percent IOP decrease (Fig. 3.5D) compared to IOP decrease magnitude (Fig. 3.5C). In Group 1, greater compressive E_{rr} was also associated with greater IOP percent decrease. E_{zz}, $E_{\theta\theta}$, E_{rz}, $E_{\theta z}$, $E_{r\theta}$, and ALD change magnitude were not associated with percent IOP decrease.

3.6 LC Strains, ALD Change, and Baseline IOP

Linear regression analysis was conducted to investigate whether strain magnitude was related to baseline IOP. For the entire medication-change group and for Group 1, there were no significant or borderline significant associations between E_{zz}, E_{rr}, $E_{\theta\theta}$, E_{rz}, $E_{\theta z}$, or $E_{r\theta}$ with baseline IOP. Furthermore, neither E_{max}, Γ_{max}, nor ALD change was associated with baseline IOP.

3.7 LC Strains, ALD Change, and Glaucoma Damage (Average RNFL, MD, and VFI)

Linear regression analysis was used to evaluate the relationship between LC strains and ALD change with three clinically-relevant measures of glaucoma damage: average RNFL, MD, and VFI. For the entire medication-change group, greater E_{max} and greater Γ_{max} were associated with a thicker average RNFL ($R^2 = 0.174$, p = 0.048 and $R^2 = 0.180$, p = 0.043 respectively; regression). E_{rr}, $E_{\theta\theta}$, E_{rz}, $E_{r\theta}$, $E_{\theta z}$, and ALD change were not related to average RNFL. For Group 1, similar behavior was observed. Greater tensile E_{zz}, greater E_{max}, and greater Γ_{max} were associated with having a thicker average RNFL ($R^2 = 0.425$, p = 4.55E-3; $R^2 = 0.424$, p = 4.61E-3; and $R^2 = 0.286$, p = 0.027; respectively). There were no correlations between E_{max}, Γ_{max}, E_{rr}, $E_{\theta\theta}$, E_{rz}, $E_{\theta z}$, $E_{r\theta}$, or ALD change with MD. For Group 1, there were no associations between E_{max}, Γ_{max}, E_{zz}, E_{rr}, $E_{\theta\theta}$, E_{rz}, $E_{\theta z}$, $E_{r\theta}$, or ALD change and MD. In both the entire medication-change group and Group 1, there were no associations

between any of the strains or ALD change with VFI.

3.8 LC Strain Compliance Response and Glaucoma Damage (Average RNFL, MD, and VFI)

These regression tests comparing strain compliance to RNFL and visual field MD and VFI were only conducted for Group 1 because the strain compliance of Group 2 could not be computed due to the fact these groups contain eyes that did not undergo IOP change which would result in division by zero. Linear regression analysis revealed greater strain compliance responses for E_{max}, Γ_{max}, and E_{zz} with greater mean RNFL thickness for the eyes in Group 1 ($R^2 = 0.415$, p = 5.26 E-4; $R^2 = 0.262$, p = 0.036; and $R^2 = 0.376$, p = 5.26E-4; respectively) (Fig. 3.6A, Fig. 3.6D, and Fig. 3.6G; respectively). The strain compliance responses for E_{rr}, $E_{\theta\theta}$, E_{rz}, $E_{\theta z}$, $E_{r\theta}$, and ALD change were not correlated with average RNFL. For Group 1, more compliant strain response for E_{max}, Γ_{max}, and E_{zz} was associated with more negative (worse) MD. Likewise, a greater strain compliance response for E_{max} and Γ_{max} was associated with lower VFI.

3.9 Biomechanical Response (Percent IOP decrease, ALD Change, LC Strains, Strain Compliances) and Age

For the entire medication-change group, there were no significant or borderline significant associations between E_{max}, Γ_{max}, E_{zz}, E_{rr}, $E_{\theta\theta}$, E_{rz}, $E_{\theta z}$, $E_{r\theta}$, or ALD change with age. For Group 1, there was a borderline association of greater compressive E_{rr} with greater age ($R^2 = 0.229$, p = 0.052), however, this trend may be influenced by an outlier by age. This outlier had an age of 30 while the rest of the of the samples were from the eyes of patients whose

age ranged from roughly 50 to 80 years old. For Group 1, the rest of the strains (E_{max}, Γ_{max}, E_{zz}, $E_{\theta\theta}$, E_{rz}, $E_{\theta z}$, $E_{r\theta}$) and ALD change did not vary significantly with age.

For Group 1, there was a more compliant compressive E_{rr} strain response with younger age ($R^2 = 0.386$, p = 7.74E-3), however, again there was an outlier with an age of 30 years old. If this outlier were removed, it appears from Fig. 3.7B that there would be little to no correlation between E_{rr} strain compliance and age for the narrow age range. There were no associations between the strain compliance response for E_{zz}, $E_{\theta\theta}$, E_{rz}, $E_{\theta z}$, $E_{r\theta}$, E_{max}, Γ_{max}, or ALD with age. Additionally, there was no association between percent IOP decrease and age.

3.10 Glaucoma Damage (RNFL, MD, VFI) and Age

Simple linear regression tests were used to assess the relationship between three measures of glaucoma damage and age. For the entire medication-change group, neither average RNFL nor VFI were associated with age. MD was borderline associated with age such that higher MD (less damage) was associated with greater age. This trend, however, appeared to be caused by an age outlier with an age of 30 years old. For Group 1, average RNFL, MD, and VFI were not significantly related to age.

3.11 Functional Measures of Glaucoma Damage (MD and VFI) and Structural Measures of Damage (RNFL)

Simple linear regression was used to assess whether MD and VFI varied with average RNFL. Neither MD nor VFI was associated with average RNFL for the entire medication-change group or for Group 1.

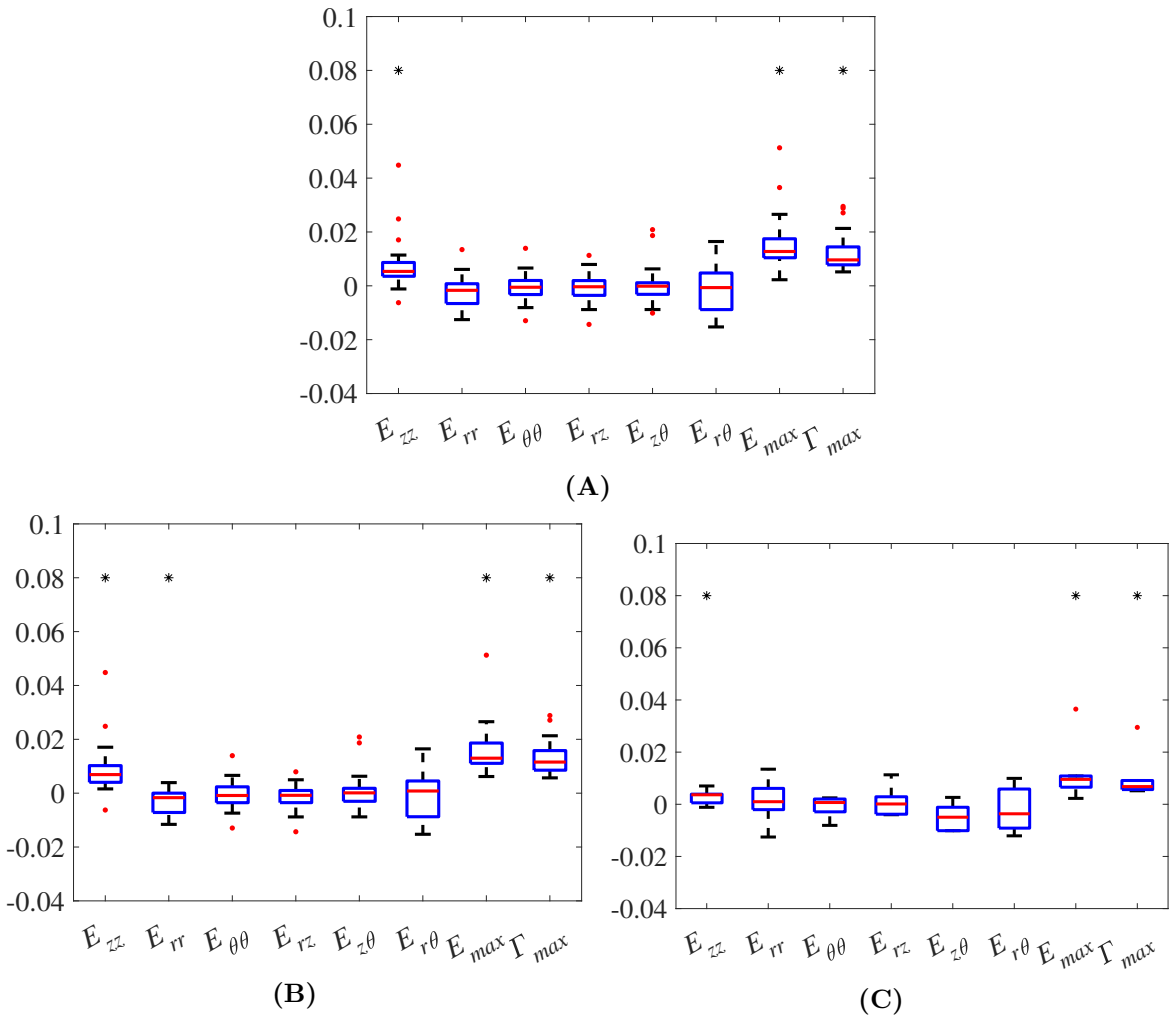

Figure 3.3: LC strains following IOP lowering from starting glaucoma medication were measured for each group using DVC and each mean strain was compared to zero using a paired t-test. An asterisk (*) indicates p-value less than or equal to 0.05. **A)** Entire medication change group. **B)** Group 1 (medication change eyes with an IOP change of at least 4 mmHg). **C)** Group 2 (medication change eyes that did not undergo a significant IOP change). IOP decrease produced by hypotensive eye drops resulted in significant tensile E_{zz} and compressive E_{rr} for Group 1. For Group 2, E_{zz} was relatively small compared to E_{zz} of Group 1 and E_{rr} was not significant.

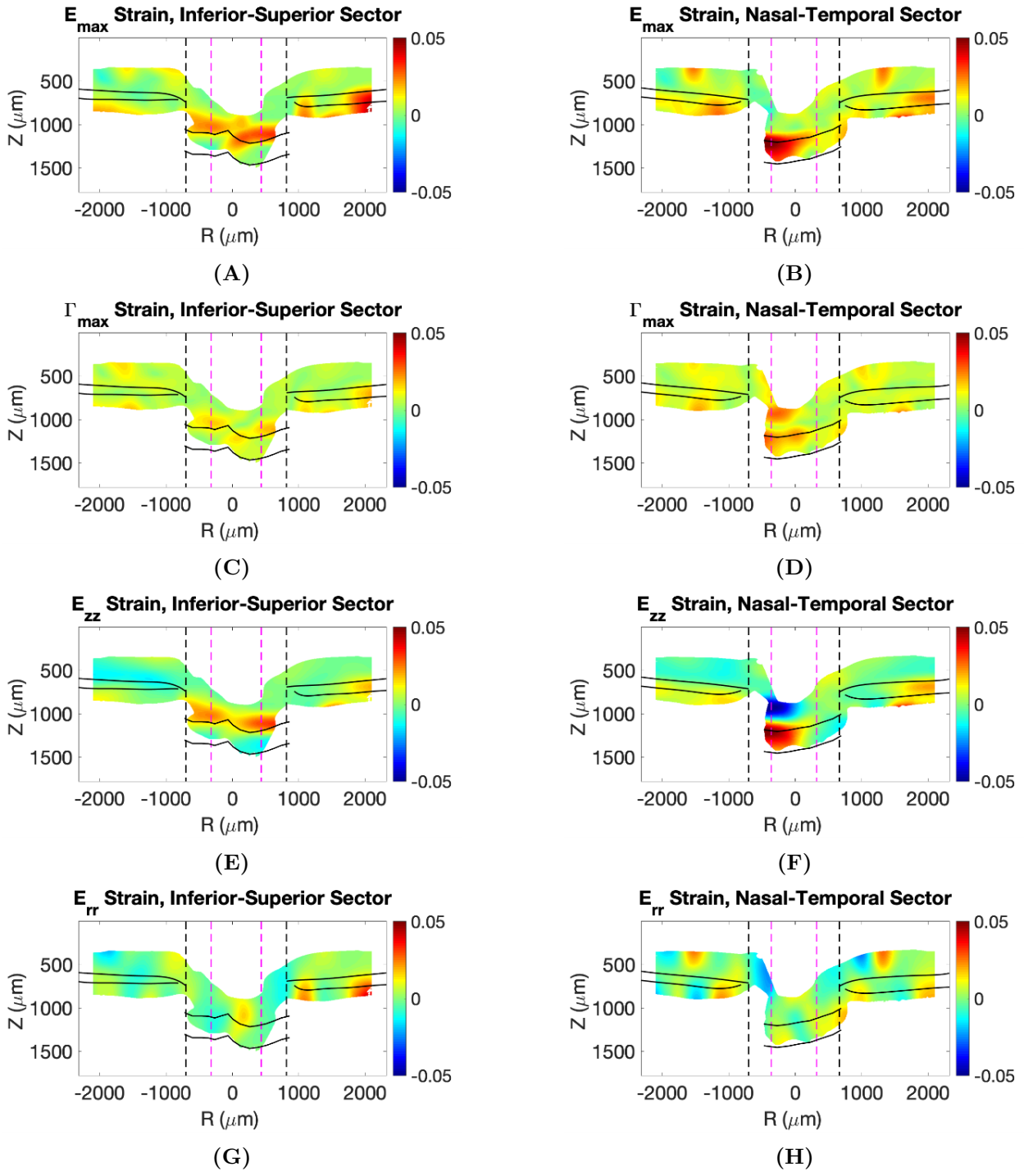

Figure 3.4: DVC strain maps of the ONH after IOP change from medication change were generated in MATLAB. These sample strain maps were taken from a Group 1 eye with an IOP decrease of -7mmHg and ALC percent correlation of 64%. **A)** E_{max} strain map for inferior-superior slice. **B)** E_{max} strain map for nasal-temporal slice. **C)** Γ_{max} strain map for inferior-superior slice. **D)** Γ_{max} strain map for nasal-temporal slice. **E)** E_{zz} strain map for inferior-superior slice. **F)** E_{zz} strain map for nasal-temporal slice. **G)** E_{rr} strain map for inferior-superior slice. **H)** E_{rr} strain map for nasal-temporal slice.

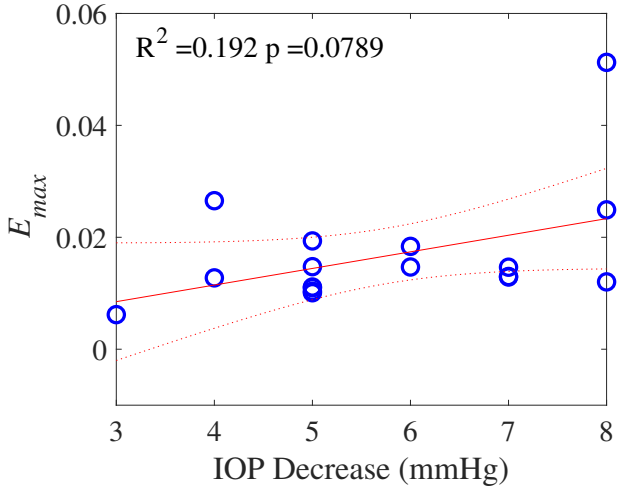
R^2 =0.192 p =0.0789
E_{max}
IOP Decrease (mmHg)

(A)

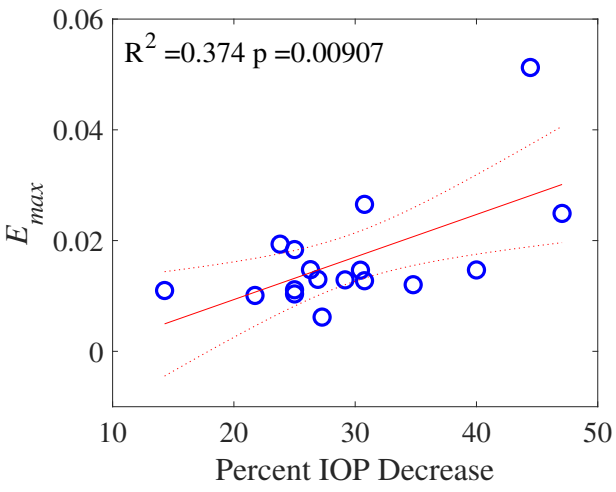
R^2 =0.374 p =0.00907
E_{max}
Percent IOP Decrease

(B)

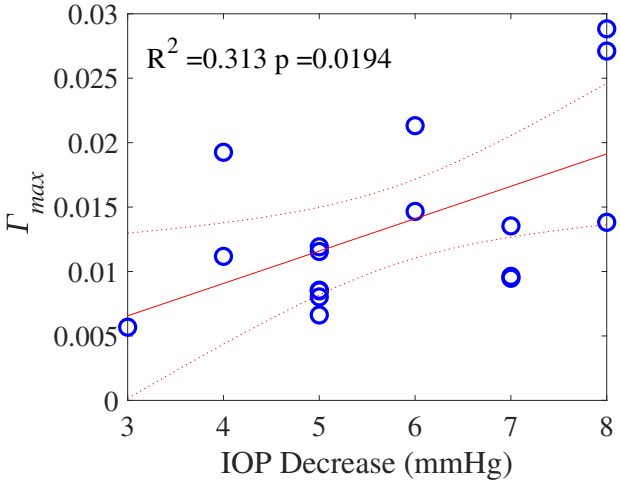
R^2 =0.313 p =0.0194
Γ_{max}
IOP Decrease (mmHg)

(C)

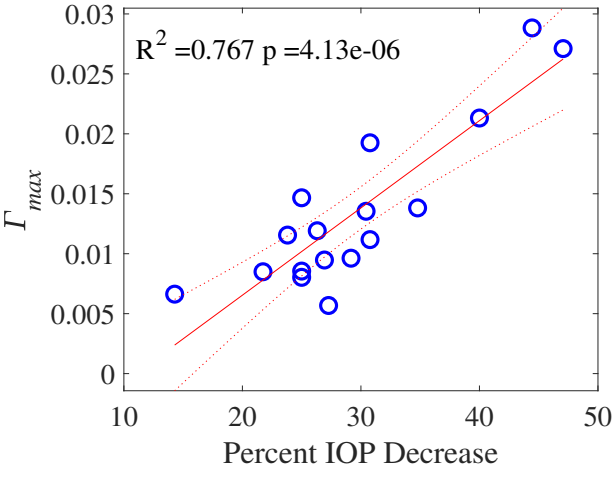
R^2 =0.767 p =4.13e-06
Γ_{max}
Percent IOP Decrease

(D)

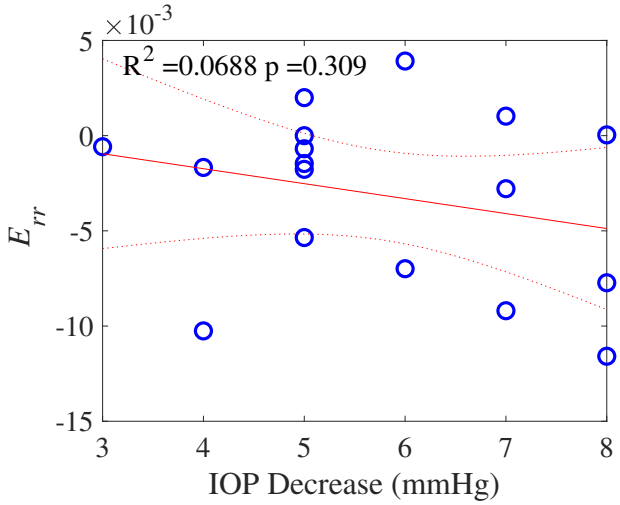
$\times 10^{-3}$
R^2 =0.0688 p =0.309
E_{rr}
IOP Decrease (mmHg)

(E)

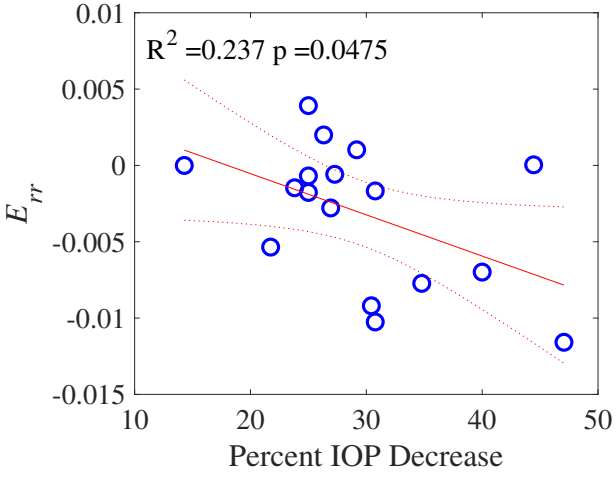
R^2 =0.237 p =0.0475
E_{rr}
Percent IOP Decrease

(F)

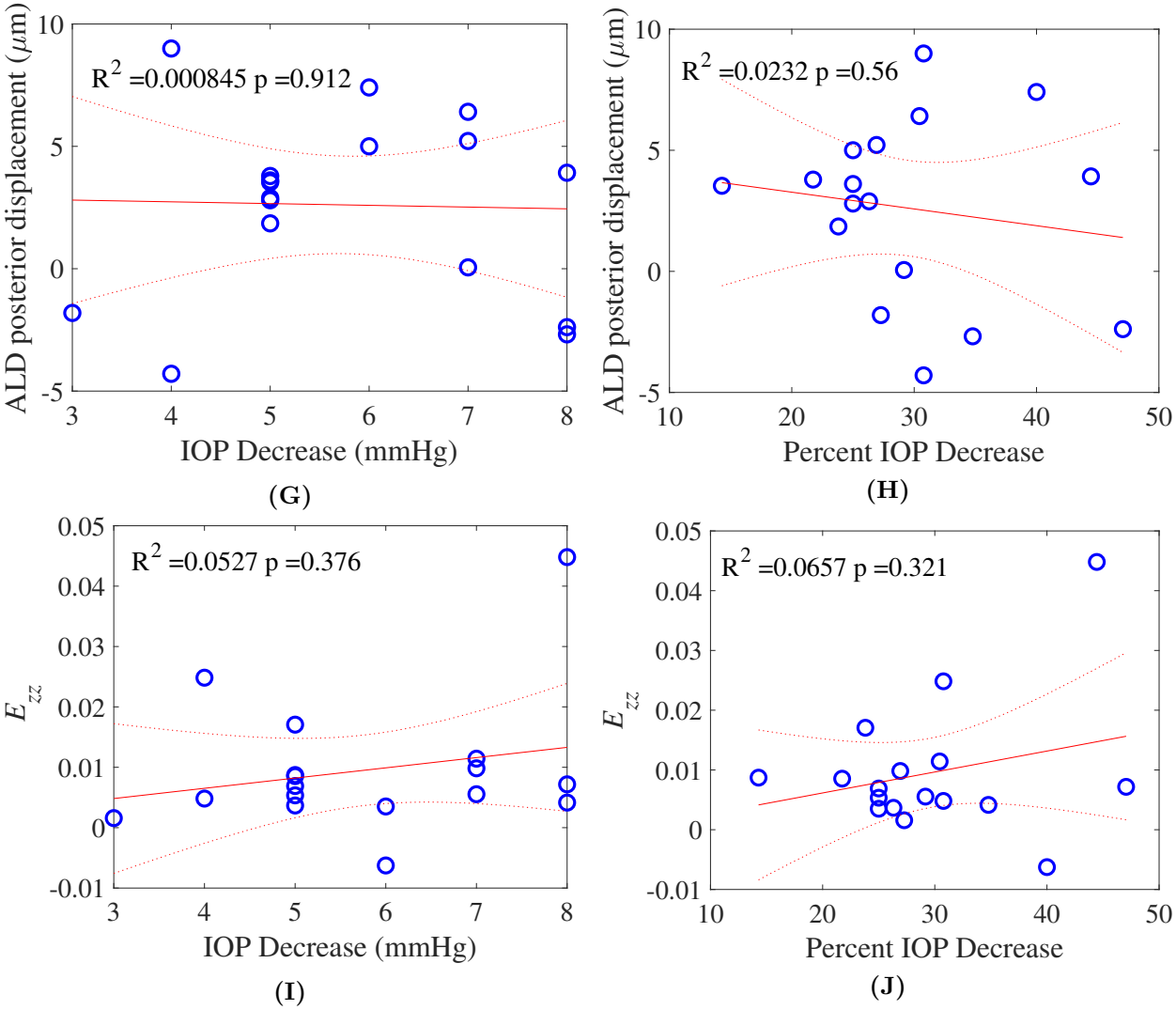

Figure 3.5: Strain magnitudes increased with greater IOP decrease and greater percent IOP decrease in the medication-change eyes of Group 1. Greater strain magnitudes were more associated with percent IOP decrease than with IOP decrease magnitude. **A)** Maximum principal strain, E_{max}, increased with greater IOP decrease. **B)** Maximum principal strain, E_{max}, increased with greater percent IOP decrease. **C)** Maximum shear strain, max, increased with greater IOP decrease. **D)** Maximum shear strain, max, increased with greater percent IOP decrease. **E)** Compressive E_{rr} increased with greater IOP decrease. **F)** Compressive E_{rr} increased with greater percent IOP decrease. **G)** ALD did not change with IOP decrease magnitude. **H)** ALD did not change with percent IOP decrease. **I)** E_{zz} did not change with IOP decrease magnitude. **J)** E_{zz} did not change with percent IOP decrease.

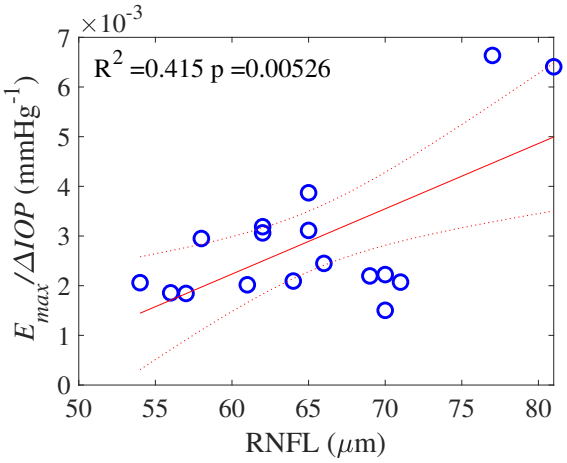
×10^-3
R^2 =0.415 p =0.00526
E_max /ΔIOP (mmHg^-1)
RNFL (μm)

(A)

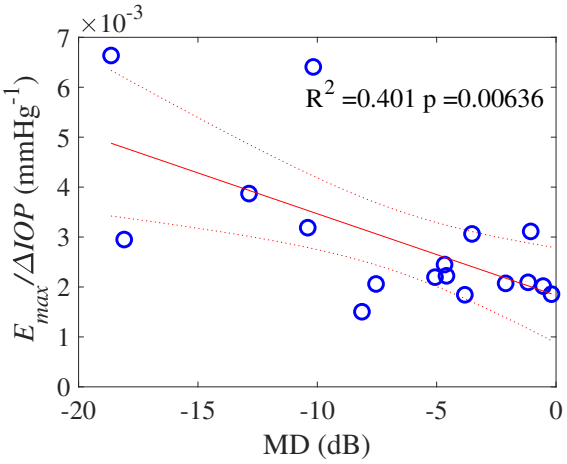
×10^-3
R^2 =0.401 p =0.00636
E_max /ΔIOP (mmHg^-1)
MD (dB)

(B)

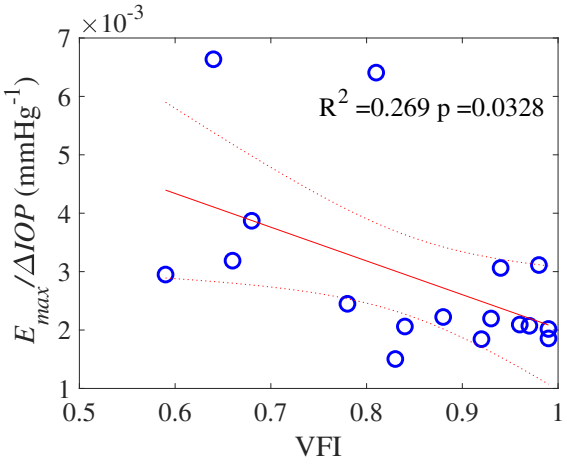
×10^-3
R^2 =0.269 p =0.0328
E_max /ΔIOP (mmHg^-1)
VFI

(C)

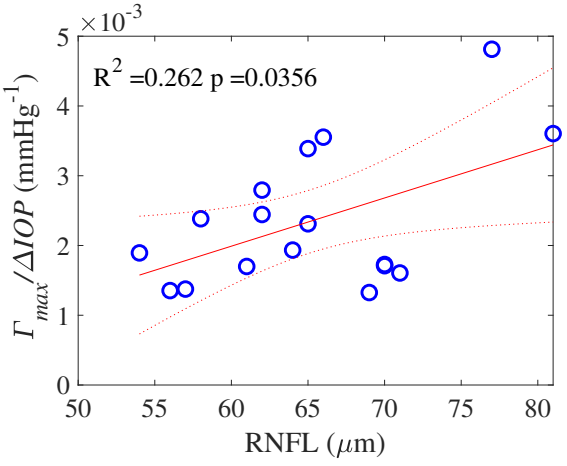
×10^-3
R^2 =0.262 p =0.0356
Γ_max /ΔIOP (mmHg^-1)
RNFL (μm)

(D)

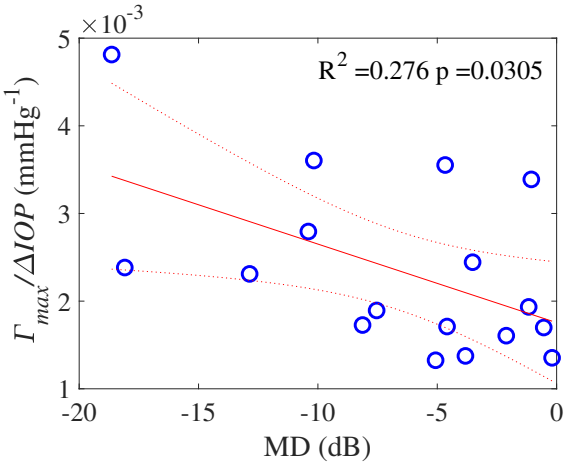
×10^-3
R^2 =0.276 p =0.0305
Γ_max /ΔIOP (mmHg^-1)
MD (dB)

(E)

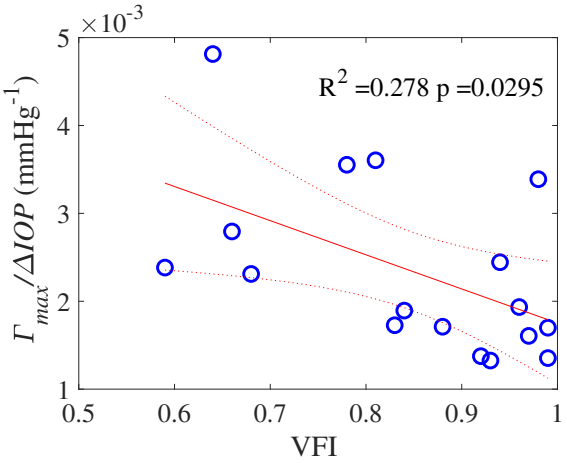
×10^-3
R^2 =0.278 p =0.0295
Γ_max /ΔIOP (mmHg^-1)
VFI

(F)

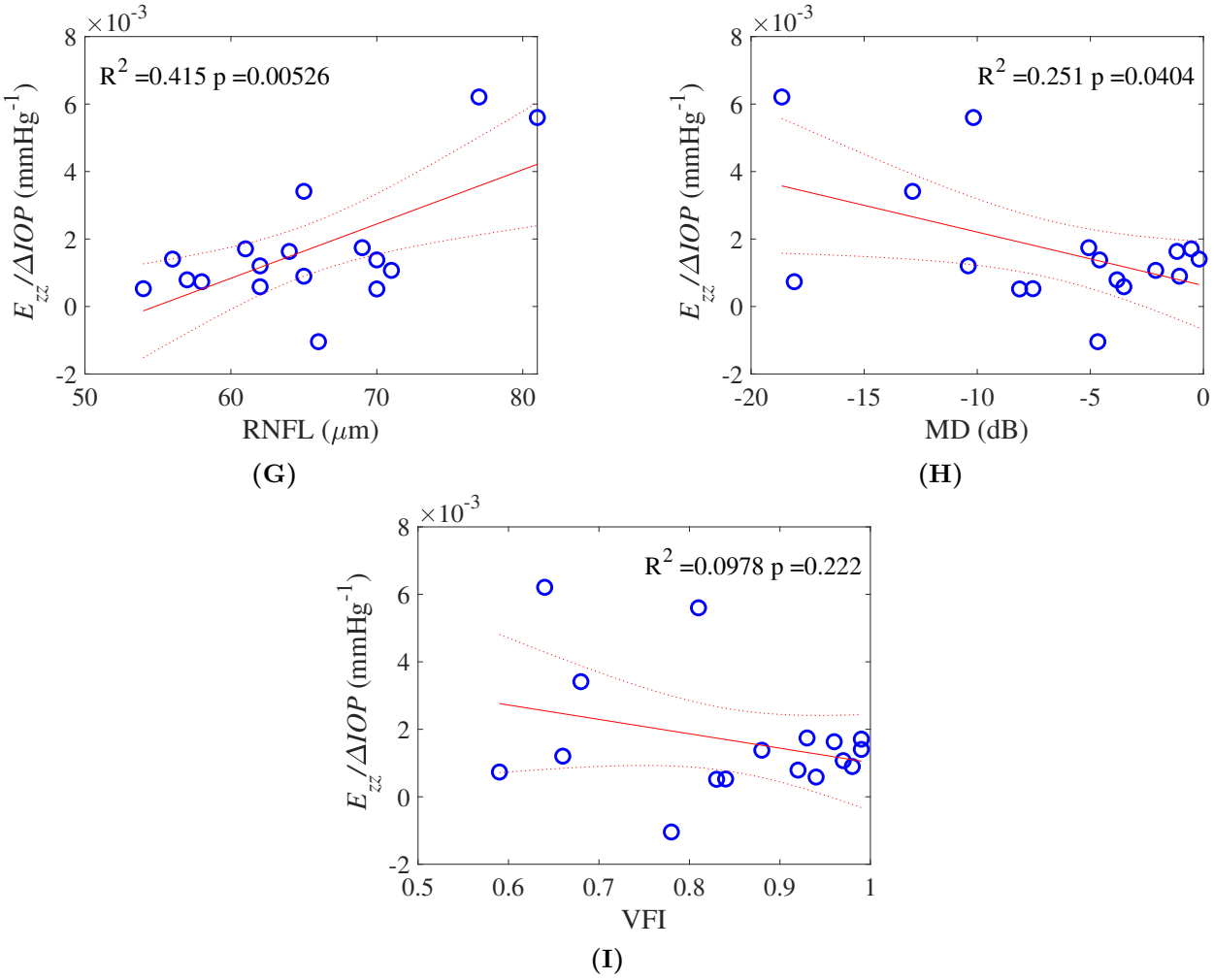

Figure 3.6: In Group 1, more compliant strain responses to IOP lowering for E_{max}, Γ_{max}, and E_{zz} were associated with thicker average RNFL (less damage), however, more compliant strain responses for E_{max}, max, and VFI were associated with more negative (worse) MD and lower (worse) VFI. **A)** Compliance of E_{max} increased with RNFL thickness. **B)** Compliance of E_{max} increased with more negative MD. **C)** Compliance of E_{max} increased with lower VFI. **D)** Compliance of Γ_{max} increased with RNFL thickness. **E)** Compliance of Γ_{max} increased with more negative MD. **F)** Compliance of Γ_{max} increased with lower VFI. **G)** Compliance of E_{zz} increased with RNFL thickness. **H)** Compliance of E_{zz} increased with more negative MD. **I)** Compliance of E_{zz} increased with lower VFI.

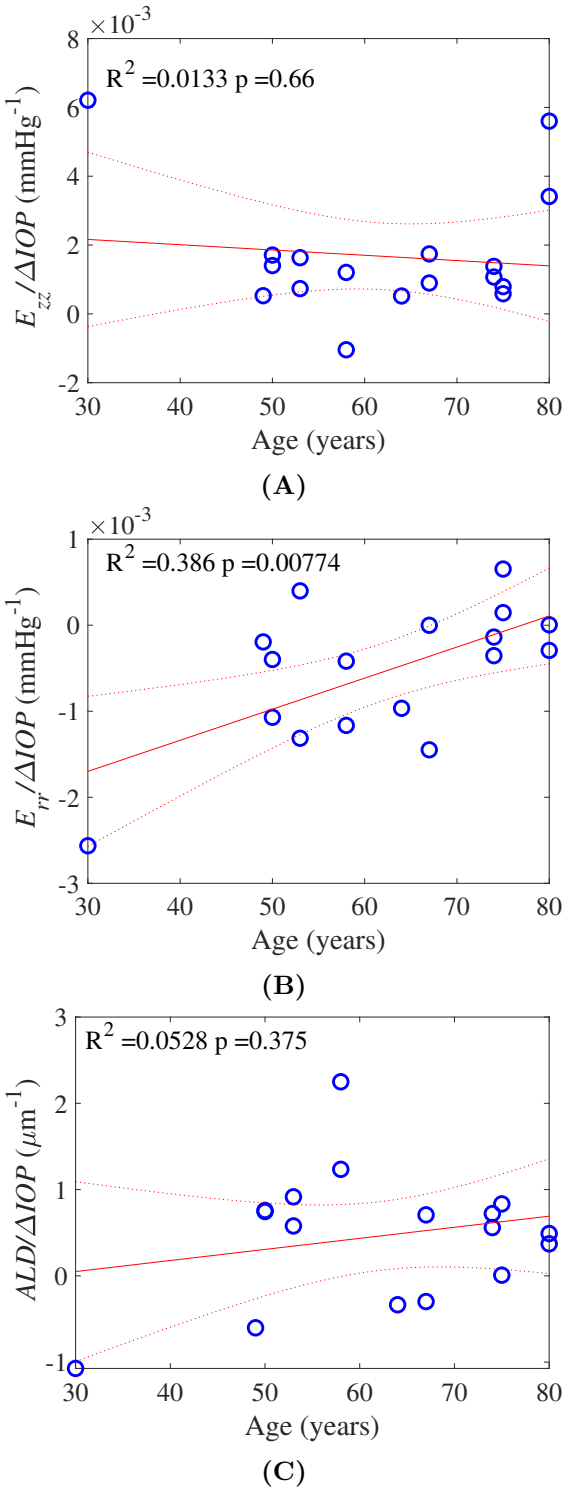

Figure 3.7: In Group 1, except for compliance of E_{rr}, the compliance response of each strain was not associated with age. Greater compliance of compressive (negative) E_{rr} was associated with younger age, however this trend appeared to be anchored by an age outlier with an age of 30 years old. **A)** The strain compliance response for E_{zz} was not associated with age. **B)** Greater compliance of compressive (negative) E_{rr} was associated with younger age. **C)** The ALD change compliance response was not associated with age.

Chapter 4

Discussion

In the present study, there were 23 medication-change eyes from 15 patients considered in total. In six eyes from five patients, IOP only decreased by 0.3 ± 0.8 mmHg. The minimal decrease in IOP for these Group 2 eyes suggests the medication type was either ineffective for the particular patient or, perhaps, suggests lack of patient compliance. For various reasons, including cost, forgetfulness, or patient reluctance (some topical eye drops may cause mild discomfort), the patient compliance rate for taking glaucoma eye drops is relatively low. The patient compliance rate tends to decrease with time, falling below 50% after one year [51]. As this was a short-term study with a treatment period of approximately one week, patient compliance was likely to be relatively higher, perhaps due to the "white-coat adherence" effect [51], with only six eyes (26 of the sample size) from five patients suggesting poor compliance.

Linear regression analysis found that greater magnitude of E_{max} and Γ_{max} was more highly correlated with greater IOP percent decrease rather than IOP decrease magnitude, suggesting the LC strain response to IOP change is not linear. This result was consistent with the findings in the study by Midgett et al. [19] and was not surprising, since IOP change alone is not normalized and it is the level of IOP rather than "elevated" IOP that is associated with greater glaucoma risk [24]. Unlike the suturelysis eyes in previous studies

by our group, there was no association between ALD change and greater strains for the medication-change eyes nor was there an association between ALD change and IOP decrease or IOP percent decrease. Additionally, there were no associations between ALD change or strains and baseline IOP for the medication-change eyes in the current study, whereas previous work by our group suggested ALD change is associated with having a lower baseline IOP [21]. This could perhaps be due to the difference in the patient population. The eyes of patients undergoing post trabeculectomy suturelysis likely had greater glaucoma damage compared to the eyes of patients subjected to IOP lowering through glaucoma eye drops; however, further statistical analysis is required to corroborate this.

In both the entire medication-change group and Group 1, IOP change related to medication-change produced significant mean tensile E_{zz} strain that exceeded baseline error but not correlation error. Due to lack of usable control data, Group 2 was used to function as a "pseudo-control" group for IOP change. After negligible IOP change (0 to 1 mmHg), the eyes in Group 2 still had a significant tensile E_{zz} strain. However, the magnitude of E_{zz} for Group 2 (0.003 ± 0.003, $p = 0.054$) was about three times smaller than E_{zz} for Group 1 (0.010 ± 0.011, $p = 0.003$). Additionally, E_{zz} for Group 2 did not exceed baseline error, unlike Group 1, suggesting the small E_{zz} strains in Group 2 may be due to error such as patient head or eye movement between images taken back-to-back, rather than IOP change. E_{rr} for Group 2 was not significantly different from zero or greater than baseline and correlation error, unlike E_{rr} for Group 1. These results suggest the methods used in the present study are valid for measuring repeatable strains in the LC. However, future studies should repeat these experiments using proper controls (i.e. eyes of patients not undergoing medication change).

The current study showed that the LC of glaucoma eyes that underwent an average IOP decrease of 6 mmHg (Group 1) due to starting hypotensive eyedrops had significant tensile E_{zz} strains and compressive E_{rr} strains. This was the expected behavior for E_{zz}, since decreasing IOP reduces the load carried by the LC along the Z-direction, allowing the

tissue to decompress and expand axially. A compressive E_{rr} implies that the LC contracted radially. This combination of strain changes would likely reduce the ONH cup to disc ratio. These findings are consistent with previous studies by our group which found that IOP reduction via post trabeculectomy suturelysis produces tensile E_{zz} and compressive E_{rr} strains in the ALC [19], [20]. Not only were the directions of E_{zz} and E_{rr} consistent for the medication-change eyes and the suturelysis eyes, but the average magnitudes of these strains were comparable, despite the medication-change eyes undergoing an average IOP decrease roughly half that of the suturelysis eyes.

The medication-change eyes in this study underwent a small, yet significant ALD change that was positive on average, indicating posterior migration of the LC surface. This was not only true for Group 1 but for all study eyes as well, which had an even smaller average IOP decrease of approximately 4 mmHg. This suggests that even relatively small IOP reductions can cause posterior movement of the anterior LC border over the course of one week. Yang et al. found that the LC migrates posteriorly in early experimental glaucoma eyes in monkeys following IOP elevation [16], whereas the present study found posterior LC migration following IOP lowering. This may be due to differences in the mechanical properties of the LC and sclera in the eyes of different species, since LC movement is mediated by the properties of both structures. The studies by Quigley et al. and Czerpak et al. found that the LC surface can move in either direction 20 minutes after IOP-lowering through suturelysis, but found no significant ALD change [21], [20]. The study by Kim et al. showed ALD depth decreases from baseline by 9.13 ± 2.05 µm after IOP-lowering through eye drops over the course of one year [15]. In other words, they found that the ALC surface moves anteriorly, towards the front of the eye [15]. In contrast, the current study found a small but significant positive ALD change, indicating LC surface movement that is posterior on average for medication-change eyes after one week. The difference in these results may be due to remodeling of the LC over time.

A key difference between the methods used in this study and those used in others was

the average time duration between acquiring pre- and post-treatment OCT images. The current study measured strains from IOP reduction over the course of one week as opposed to the studies by Czerpak et al. [20] and Midgett et al. [19] which measured strains from IOP decrease from suturelysis or IOP increase from tight-fitting goggles after 20 minutes. From a biomechanical standpoint, this suggests that time after IOP change may be another independent variable.

The one week between each imaging session for the eyes studied here could allow for slowly increasing strains assuming a relatively constant load (stable IOP after lowering), implying a creep response characteristic of viscoelastic materials. Biological tissues are viscoelastic in nature, meaning their deformation response behaves partly like a viscous fluid and partly like an elastic solid. Creep is the slow increase in strain with time when the loading conditions are held constant. The LC E_{zz} strain (0.010 $\pm$ 0.011, p = 0.003) and E_{rr} strain (0.003 $\pm$ 0.005, p = 0.012) magnitudes for the Group 1 eyes were comparable to the LC E_{zz} (0.0094 $\pm$ .0012, p = 0.012) and E_{rr} (-0.0019 $\pm$ .0033, p = 0.0043) for the suturelysis study by Czerpak et al. [20], despite having roughly half the average IOP decrease of the suturelysis eyes. This could be explained by the event of a creep response occurring in the Group 1 eyes, which were subjected to an assumed constant load (stable IOP after lowering) over a one-week period as opposed to a 20-minute period, in which, likely only the elastic strain response occurred. A creep response to IOP lowering suggests that the LC is a viscoelastic material.

One intriguing result from the current study was that greater strains and more compliant strain response were associated with thicker RNFL for the medication-change eyes. This was the opposite relationship observed for the suturelysis eyes, in which more compliant strain response was associated with thinner RNFL (more damage) [20]. However, consistent with the findings from the suturelysis strain response study, greater strains and more compliant strain response in the medication-change eyes were associated with lower VFI and more negative MD. Close inspection of Fig. 3.6A, Fig. 3.6D, and Fig. 3.6G revealed that there

were two outliers at a higher compliance and greater RNFL thickness compared to the rest of the samples. These outliers appeared to heavily influence the slope of the regression line. If the outliers were to be removed, a linear relationship between RNFL thickness and strain compliance appears unlikely.

The medication-change eyes in the study by Kim et al. found greater reduction of LC curvature was associated with younger age [15]. The present study did not measure LC curvature but found ALD change was not significantly correlated with age. E_{rr} strain was more compliant with lower age; however it was unclear whether this trend was truly significant, since it appeared to be anchored by an age outlier with a much younger age and more compliant E_{rr} response (Fig. 3.7B).

There were numerous limitations to the present study. First, this study lacked a control group. In other words, to further validate the methods used in the current study for measuring LC strains in the eyes of patients undergoing medication change, a control group consisting of patients who did not start or stop glaucoma medication should have been included. Instead, the eyes in Group 2, which still underwent medication-change but did not undergo IOP change, were used in place as "pseudo-controls". Furthermore, the image quality of the OCT scans varied greatly which resulted in images for seven eyes being excluded due to poor image quality. Poor image quality typically was due to high noise and poor contrast, rendering these images unsuitable for DVC analysis. However, due to lack of samples, many images with marginal image quality were retained which likely contributed to higher variability in ALC percent correlation. A few samples were excluded due to poor visibility of the LC or poor image registration. Some OCT image volumes had great focus, high contrast, and low noise, but the LC was not visible due to the presence of shadows cast by overlying blood vessels from individual anatomy. Not only were these images difficult to hand-mark, but the resulting ALC percent correlation was too low (below 20%) to obtain meaningful results. Additionally, there were some OCT images where the LC region was lost due to the image being cut off at the bottom. In terms of image registration, there were

some image pairs where the orientation of the ONH was highly misaligned and appeared to "jump" around. These samples were excluded, as they would likely result in false DVC displacements/strains.

In terms of imaging, since the medication-change eyes in this study were imaged before and after treatment on separate days, it is unlikely that the imaging setup was identical at both imaging sessions. The height of the imaging table, chin rest, and patient's head position likely differed at these sessions which could result in false movement of the ONH from before and after images, contributing to increased error.

In terms of the patient demographic, the included eyes were biased towards patients with mild glaucoma damage (MD better than -6 dB). The entire medication-change group included 15 eyes with mild glaucoma, 5 eyes with moderate glaucoma, and 3 eyes with severe damage. Additionally, the patient demographic was biased towards female patients. There were nearly twice as many medication-change eyes from female patients than from male patients.

In terms of statistical analysis, it was assumed the data all followed normal distributions, however, this was not verified. A considerable weakness of the present study was that it did not account for inter-eye correlation. This effect may introduce more bias since a left and right eye from one patient would be expected to respond to IOP change more similarly than a left and right eye from two different patients.

Chapter 5

Conclusion

In conclusion, this was is original pilot study that, to the best of the author's knowledge, was the first study to measure the short-term *in vivo* biomechanical response of the human lamina cribrosa to IOP change resulting from glaucoma medication change. Through a method based on digital volume correlation of radial OCT scans developed by the Nguyen Lab at Johns Hopkins University, this pilot study demonstrated that the methods used show promise to quantify significant, repeatable, *in vivo* LC strains and ALD change as a result of IOP change in the eyes of patients subjected to glaucoma medication change. The current study showed that measuring the *in vivo* biomechanical response to IOP change from starting or stopping hypotensive eye drops can be performed in a clinical setting through noninvasive and low risk procedures. If conducted on a greater scale, the collection and analysis of more patient-specific biomechanical response data may shed light on less-well-understood phenomena of glaucoma. Ultimately, these patient-specific biomechanical responses may serve as unique biomarkers for glaucoma with the potential to improve patient diagnosis and care.

Chapter 6

Future Work

The results obtained in this pilot study provide both proof of concept and preliminary data for future studies. Future work may include repeating this study on a larger scale to demonstrate reproducible strains using the method described in the current study. A larger scale study would include an adequately-sized control group to validate the experimental group findings and method. Additionally, longer term follow-up studies to assess strain in the eyes in the current study are recommended to better understand the complex biomechanical strain and remodeling response of the LC to IOP change over time. Longer term studies conducted at various intervals (e.g. 1 month, 3 months, 6 months, 1 year), may allow for better characterization of the viscoelastic strain and remodeling response of the LC to IOP change in the eyes undergoing glaucoma medication change.

In terms of analysis, it is highly recommended that future related studies account for inter-eye correlation effects to avoid bias which could be done using more sophisticated methods such as linear mixed models. Additionally, it is recommended to seek a means of quantifying image quality, registration, and visibility of the LC in OCT scans, perhaps through machine learning algorithms. Quantification of these parameters would allow a minimum threshold to be set that will ensure higher quality data and less reliance on subjective measures for excluding samples based on "image quality". Future work may investigate the

relationship between patient medication compliance and the biomechanical response of the optic nerve head. Future work may also seek to measure and analyze strains beyond the ALC for medication-change eyes, such as those in the PPS, since the biomechanical response to IOP change is mediated by the LC acting together with the PPS.

Appendix A

A.1 Acronym Glossary

Table A.1: A glossary of acronyms used throughout this study in alphabetical order

Acronym	Definition
1D	One-dimensional
2D	Two-dimensional
3D	Three-dimensional
ALC	Anterior lamina cribrosa
ALD	Anterior lamina depth
CLAHE	Contrast limited adaptive histogram equalization
DIC	Digital image correlation
DVC	Digital volume correlation
IOP	Intraocular pressure
LC	Lamina cribrosa
MD	Mean deviation
OCT	Optical coherence tomography
ONH	Optic nerve head
POAG	Primary open-angle glaucoma
RGC	Retinal ganglion cell
RNFL	Retinal nerve fiber layer
VFI	Visual field index

A.2 Specimen Information

Table A.2: Further patient demographic information, medication type, and time interval between imaging sessions were recorded. The study specimens were subjected to IOP lowering to reach target IOP through the administration of hypotensive eye drops. *Eye 10 stopped eye drops. All other medication-change eyes were starting new glaucoma medication. The following abbreviations were used for patient sex: F = female, M = male. The different categories of patient race were abbreviated as: A = Asian, AA = African American, W = White.

Eye	Age (years)	Sex	Race	MD	Baseline IOP	IOP Change (mmHg)	Rx Type	Interval (days)
1	75	F	W	-3.82	24	-7	Eye drops	7
2	75	F	W	-3.52	24	-6	Eye drops	7
3	53	M	W	-1.17	23	-7	Eye drops	7
4	50	F	W	-0.54	23	-5	Eye drops	7
5	50	F	W	-0.19	26	-7	Eye drops	7
6	70	F	W	1.4	10	0	Eye drops	7
7	70	F	W	1.4	11	-1	Eye drops	7
8	53	M	W	-18.09	19	-5	Eye drops	7
9	64	M	W	-8.13	23	-8	Eye drops	7
10	53	M	A	-12.1	12	-1	Eye drops*	7
11	49	F	A	-7.54	11	-3	Eye drops	10
12	49	F	A	-10.48	10	-1	Eye drops	10
13	58	M	W	-4.67	15	-6	Eye drops	5
14	58	M	W	-10.4	13	-4	Eye drops	5
15	67	F	AA	-1.06	17	-8	Eye drops	7
16	30	F	W	-18.64	13	-4	Oral	7
17	80	F	AA	-12.86	21	-5	Eye drops	7
18	80	F	AA	-10.17	18	-8	Eye drops	7
19	74	F	W	-2.11	20	-5	Eye drops	10
20	74	F	W	-4.59	20	-5	Eye drops	10
21	62	F	AA	-2.04	9	1	Eye drops	7
22	67	M	AA	-5.07	35	-5	Eye drops	7
23	67	M	AA	-3.7	23	0	Eye drops	7

A.3 Strain Compliance Equations

Strain compliances for ALD change, E_{rr}, E_{zz}, $E_{\theta\theta}$, E_{rz}, $E_{\theta z}$, $E_{r\theta}$, maximum principal strain (E_{max}), and maximum shear strain (Γ_{max}) were obtained by dividing each strain by change in IOP:

$$\frac{\Delta ALD}{\Delta IOP} \tag{A.1}$$

$$\frac{E_{rr}}{\Delta IOP} \tag{A.2}$$

$$\frac{E_{zz}}{\Delta IOP} \tag{A.3}$$

$$\frac{E_{\theta\theta}}{\Delta IOP} \tag{A.4}$$

$$\frac{E_{rz}}{\Delta IOP} \tag{A.5}$$

$$\frac{E_{\theta z}}{\Delta IOP} \tag{A.6}$$

$$\frac{E_{max}}{\Delta IOP} \tag{A.7}$$

$$\frac{\Gamma_{max}}{\Delta IOP} \tag{A.8}$$

A.4 Image Processing Code (CLAHE and Gamma Filter)

The following code written for ImageJ Fiji used CLAHE and a gamma filter to process OCT image volumes in preparation for DVC:

```
getDimensions(width, height, channels, slices, frames);
for ( s=1; s ≤ slices; s++ )
{
Stack.setSlice(s);
//ClAHE
blocksize = 14;
histogram_bins = 256;
maximum_slope = 3.5;
mask = "*None*";
parameters =
"blocksize=" + blocksize +
" histogram=" + histogram_bins +
" maximum=" + maximum_slope +
" mask=" + mask;
run( "Enhance Local Contrast (CLAHE)", parameters );
//Gamma Shift
run("Gamma...", "value=1.75");
}
```

Bibliography

[1] Dan Midgett. "Measuring the Full-Field Inflation Response of the Optic Nerve Head". en. PhD thesis. Baltimore, MD, May 2018.

[2] A Foster and S Resnikoff. "The impact of Vision 2020 on global blindness". en. In: *Eye* 19.10 (Oct. 2005), pp. 1133–1135. ISSN: 0950-222X, 1476-5454. DOI: 10.1038/sj.eye.6701973.

[3] Robert N. Weinreb, Tin Aung, and Felipe A. Medeiros. "The Pathophysiology and Treatment of Glaucoma: A Review". en. In: *JAMA* 311.18 (May 14, 2014), p. 1901. ISSN: 0098-7484. DOI: 10.1001/jama.2014.3192.

[4] Karen Allison, Deepkumar Patel, and Omobolanle Alabi. "Epidemiology of Glaucoma: The Past, Present, and Predictions for the Future". en. In: *Cureus* (Nov. 24, 2020). [Online; accessed 2022-06-20]. ISSN: 2168-8184. DOI: 10.7759/cureus.11686. URL: https://www.cureus.com/articles/42672-epidemiology-of-glaucoma-the-past-present-and-predictions-for-the-future.

[5] Harry A Quigley, Stuart J McKinnon, Donald J Zack, Mary Ellen Pease, Lisa A Kerrigan, Danielle F Kerrigan, and Rebecca S Mitchell. "Retrograde Axonal Transport of BDNF in Retinal Ganglion Cells Is Blocked by Acute IOP Elevation in Rats". en. In: 41.11 (2000), p. 7.

[6] Luis E Vazquez and Linda Y Huang. "RNFL ANALYSIS IN THE DIAGNOSIS OF GLAUCOMA". en. In: (), p. 2.

[7] Igor I Bussel, Gadi Wollstein, and Joel S Schuman. "OCT for glaucoma diagnosis, screening and detection of glaucoma progression". en. In: *British Journal of Ophthalmology* 98.Suppl 2 (July 2014), pp. ii15–ii19. ISSN: 0007-1161, 1468-2079. DOI: 10.1136/bjophthalmol-2013-304326.

[8] Harry A. Quigley and Frances E. Cone. "Development of diagnostic and treatment strategies for glaucoma through understanding and modification of scleral and lamina cribrosa connective tissue". en. In: *Cell and Tissue Research* 353.2 (Aug. 2013), pp. 231–244. ISSN: 0302-766X, 1432-0878. DOI: 10.1007/s00441-013-1603-0.

[9] John C Morrison, Kristina B Nylander, Andreas K Lauer, and Elaine Johnson. "Glaucoma Drops Control Intraocular Pressure and Protect Optic Nerves in a Rat Model of Glaucoma". en. In: (), p. 6.

[10] Michael A. Kass, Dale K. Heuer, Eve J. Higginbotham, Chris A. Johnson, John L. Keltner, J. Philip Miller, II Parrish Richard K., M. Roy Wilson, Mae O. Gordon, and for the Ocular Hypertension Treatment Study Group. "The Ocular Hypertension Treatment Study: A Randomized Trial Determines That Topical Ocular Hypotensive Medication Delays or Prevents the Onset of Primary Open-Angle Glaucoma". In: *Archives of Ophthalmology* 120.6 (June 2002). _eprint: https://jamanetwork.com/journals/jamaophthalmology/article pp. 701–713. ISSN: 0003-9950. DOI: 10.1001/archopht.120.6.701. URL: https://doi.org/10.1001/archopht.120.6.701.

[11] L. P. Cohen and L. R. Pasquale. "Clinical Characteristics and Current Treatment of Glaucoma". en. In: *Cold Spring Harbor Perspectives in Medicine* 4.6 (June 1, 2014), a017236–a017236. ISSN: 2157-1422. DOI: 10.1101/cshperspect.a017236.

[12] Alexander K. Schuster, Carl Erb, Esther M. Hoffmann, Thomas Dietlein, and Norbert Pfeiffer. "The Diagnosis and Treatment of Glaucoma". en. In: *Deutsches Ärzteblatt international* (Mar. 27, 2020). [Online; accessed 2022-10-31]. ISSN: 1866-0452. DOI:

10.3238/arztebl.2020.0225. URL: https://www.aerzteblatt.de/10.3238/arztebl.2020.0225.

[13] Harry A Quigley, Robert W Nickells, Lisa A Kerrigan, Mary E Pease, Diane J Thibault, and Donald J Zack. "Retinal Ganglion Cell Death in Experimental Glaucoma and After Axotomy Occurs by Apoptosis". en. In: (), p. 13.

[14] Li Guo, Stephen E. Moss, Robert A. Alexander, Robin R. Ali, Frederick W. Fitzke, and M. Francesca Cordeiro. "Retinal Ganglion Cell Apoptosis in Glaucoma Is Related to Intraocular Pressure and IOP-Induced Effects on Extracellular Matrix". en. In: *Investigative Opthalmology Visual Science* 46.1 (Jan. 1, 2005), p. 175. ISSN: 1552-5783. DOI: 10.1167/iovs.04-0832.

[15] Jeong-Ah Kim, Seung Hyen Lee, Dong Hwan Son, Tae-Woo Kim, Eun Ji Lee, Michaël J. A. Girard, and Jean Martial Mari. "Morphologic Changes in the Lamina Cribrosa Upon Intraocular Pressure Lowering in Patients With Normal Tension Glaucoma". en. In: *Investigative Opthalmology Visual Science* 63.2 (Feb. 11, 2022), p. 23. ISSN: 1552-5783. DOI: 10.1167/iovs.63.2.23.

[16] Hongli Yang, Galen Williams, J. Crawford Downs, Ian A. Sigal, Michael D. Roberts, Hilary Thompson, and Claude F. Burgoyne. "Posterior (Outward) Migration of the Lamina Cribrosa and Early Cupping in Monkey Experimental Glaucoma". en. In: *Investigative Opthalmology Visual Science* 52.10 (Sept. 8, 2011), p. 7109. ISSN: 1552-5783. DOI: 10.1167/iovs.11-7448.

[17] Sung Chul Park, John Brumm, Rafael L. Furlanetto, Camila Netto, Yiyi Liu, Celso Tello, Jeffrey M. Liebmann, and Robert Ritch. "Lamina Cribrosa Depth in Different Stages of Glaucoma". en. In: *Investigative Opthalmology Visual Science* 56.3 (Mar. 31, 2015), p. 2059. ISSN: 1552-5783. DOI: 10.1167/iovs.14-15540.

[18] Eun Ji Lee, Tae-Woo Kim, and Robert N. Weinreb. "Reversal of Lamina Cribrosa Displacement and Thickness after Trabeculectomy in Glaucoma". en. In: *Ophthalmology*

119.7 (July 2012), pp. 1359–1366. ISSN: 01616420. DOI: 10.1016/j.ophtha.2012.01.034.

[19] Dan E. Midgett, Harry A. Quigley, and Thao D. Nguyen. "In vivo characterization of the deformation of the human optic nerve head using optical coherence tomography and digital volume correlation". en. In: *Acta Biomaterialia* 96 (Sept. 2019), pp. 385–399. ISSN: 17427061. DOI: 10.1016/j.actbio.2019.06.050.

[20] Cameron A. Czerpak, Michael Saheb Kashaf, Brandon K. Zimmerman, Harry A. Quigley, and Thao D. Nguyen. "The Strain Response to Intraocular Pressure Decrease in the Lamina Cribrosa of Patients with Glaucoma". en. In: *Ophthalmology Glaucoma* (July 2022), S258941962200120X. ISSN: 25894196. DOI: 10.1016/j.ogla.2022.07.005.

[21] Harry Quigley, Karun Arora, Sana Idrees, Francisco Solano, Sahar Bedrood, Christopher Lee, Joan Jefferys, and Thao D. Nguyen. "Biomechanical Responses of Lamina Cribrosa to Intraocular Pressure Change Assessed by Optical Coherence Tomography in Glaucoma Eyes". en. In: *Investigative Opthalmology Visual Science* 58.5 (June 20, 2017), p. 2566. ISSN: 1552-5783. DOI: 10.1167/iovs.16-21321.

[22] Michaël J.A. Girard, Meghna R. Beotra, Khai Sing Chin, Amanjeet Sandhu, Monica Clemo, Eleni Nikita, Deborah S. Kamal, Maria Papadopoulos, Jean Martial Mari, Tin Aung, and Nicholas G. Strouthidis. "In Vivo 3-Dimensional Strain Mapping of the Optic Nerve Head Following Intraocular Pressure Lowering by Trabeculectomy". en. In: *Ophthalmology* 123.6 (June 2016), pp. 1190–1200. ISSN: 01616420. DOI: 10.1016/j.ophtha.2016.02.008.

[23] Meghna R. Beotra, Xiaofei Wang, Tin A. Tun, Liang Zhang, Mani Baskaran, Tin Aung, Nicholas G. Strouthidis, and Michaël J. A. Girard. "In Vivo Three-Dimensional Lamina Cribrosa Strains in Healthy, Ocular Hypertensive, and Glaucoma Eyes Following Acute

Intraocular Pressure Elevation". en. In: *Investigative Opthalmology Visual Science* 59.1 (Jan. 16, 2018), p. 260. ISSN: 1552-5783. DOI: 10.1167/iovs.17-21982.

[24] Harry A. Quigley. "The contribution of the sclera and lamina cribrosa to the pathogenesis of glaucoma". en. In: *Progress in Brain Research*. Vol. 220. DOI: 10.1016/bs.pbr.2015.04.003. Elsevier, 2015, pp. 59–86. ISBN: 978-0-444-63566-2. URL: https://linkinghub.elsevier.com/retrieve/pii/S0079612315000606.

[25] Ricardo Y. Abe, Carolina P. B. Gracitelli, Alberto Diniz-Filho, Andrew J. Tatham, and Felipe A. Medeiros. "Lamina Cribrosa in Glaucoma: Diagnosis and Monitoring". en. In: *Current Ophthalmology Reports* 3.2 (June 2015), pp. 74–84. ISSN: 2167-4868. DOI: 10.1007/s40135-015-0067-7.

[26] Claude F. Burgoyne. "A biomechanical paradigm for axonal insult within the optic nerve head in aging and glaucoma". en. In: *Experimental Eye Research* 93.2 (Aug. 2011), pp. 120–132. ISSN: 00144835. DOI: 10.1016/j.exer.2010.09.005.

[27] J Crawford Downs, Michael D. Roberts, and Claude F. Burgoyne. "Mechanical Environment of the Optic Nerve Head in Glaucoma". en. In: *Optometry and Vision Science* 85.6 (June 2008), E425–E435. ISSN: 1040-5488. DOI: 10.1097/OPX.0b013e31817841cb.

[28] Young H. Kwon, John H. Fingert, Markus H. Kuehn, and Wallace L.M. Alward. "Primary Open-Angle Glaucoma". en. In: *New England Journal of Medicine* 360.11 (Mar. 12, 2009), pp. 1113–1124. ISSN: 0028-4793, 1533-4406. DOI: 10.1056/NEJMra0804630.

[29] Sung Chul Park. "In Vivo Evaluation of Lamina Cribrosa Deformation in Glaucoma:" en. In: *Journal of Glaucoma* 22 (2013), S29–S31. ISSN: 1057-0829. DOI: 10.1097/IJG.0b013e3182934a7b.

[30] H. A. Quigley and E. M. Addicks. "Regional Differences in the Structure of the Lamina Cribrosa and Their Relation to Glaucomatous Optic Nerve Damage". en. In: *Archives of Ophthalmology* 99.1 (Jan. 1, 1981), pp. 137–143. ISSN: 0003-9950. DOI: 10.1001/archopht.1981.03930010139020.

[31] Harry A Quigley, Earl M Addicks, W Richard Green, and A E Maumenee. "Optic Nerve Damage in Human Glaucoma: II. The Site of Injury and Susceptibility to Damage". en. In: (), p. 15.

[32] Harry A. Quigley, Rebecca M. Hohman, Earl M. Addicks, Robert W. Massof, and W. Richard Green. "Morphologic Changes in the Lamina Cribrosa Correlated with Neural Loss in Open-Angle Glaucoma". en. In: *American Journal of Ophthalmology* 95.5 (May 1983), pp. 673–691. ISSN: 00029394. DOI: 10.1016/0002-9394(83)90389-6.

[33] J. Albon. "Age related compliance of the lamina cribrosa in human eyes". en. In: *British Journal of Ophthalmology* 84.3 (Mar. 1, 2000), pp. 318–323. ISSN: 00071161. DOI: 10.1136/bjo.84.3.318.

[34] *iCare TA01i Tonometer – quick and easy IOP measurements.* [Online; accessed 2022-06-23]. URL: https://www.icare-world.com/wp-content/uploads/2021/10/iCare_TA01i_broch_HR130921.pdf.

[35] N. M. Shoshani, G. T. Liu, and A. Shrivastava. "Reliability and Reproducibility of IOLMaster Optical Biometry Measurements for Cataract Surgery Preoperative Assessment, Pre- and Post-Dilation and Examination". In: *Investigative Ophthalmology Visual Science* 51.13 (Apr. 17, 2010), pp. 5409–5409. ISSN: 1552-5783.

[36] Silke Aumann, Sabine Donner, Jörg Fischer, and Frank Müller. "Optical Coherence Tomography (OCT): Principle and Technical Realization". en. In: *High Resolution Imaging in Microscopy and Ophthalmology.* Ed. by Josef F. Bille. DOI: 10.1007/978-3-030-16638-0_3. Cham: Springer International Publishing, 2019, pp. 59–85. ISBN: 978-3-030-16637-3. URL: http://link.springer.com/10.1007/978-3-030-16638-0_3.

[37] David Huang. *OCT Terminology — Demystified! A pioneer of the technology provides a translation of the latest jargon.* [Online; accessed 2022-11-30]. Apr. 1, 2009. URL: https://www.ophthalmologymanagement.com/issues/2009/april-2009/oct-terminology-demystified.

[38] Joel S. Schuman. "Spectral Domain Optical Coherence Tomography for Glaucoma (An AOS Thesis)". In: *Transactions of the American Ophthalmological Society* 106 (Dec. 2008). PMID: 19277249 PMCID: PMC2646438, pp. 426–458. ISSN: 0065-9533.

[39] Christopher Kai-shun Leung, Carol Yim-lui Cheung, Robert N. Weinreb, Gary Lee, Dusheng Lin, Chi Pui Pang, and Dennis S. C. Lam. "Comparison of Macular Thickness Measurements between Time Domain and Spectral Domain Optical Coherence Tomography". In: *Investigative Ophthalmology Visual Science* 49.11 (Nov. 1, 2008), pp. 4893–4897. ISSN: 1552-5783. DOI: 10.1167/iovs.07-1326.

[40] Johannes Schindelin, Ignacio Arganda-Carreras, Erwin Frise, Verena Kaynig, Mark Longair, Tobias Pietzsch, Stephan Preibisch, Curtis Rueden, Stephan Saalfeld, Benjamin Schmid, Jean-Yves Tinevez, Daniel James White, Volker Hartenstein, Kevin Eliceiri, Pavel Tomancak, and Albert Cardona. "Fiji: an open-source platform for biological-image analysis". en. In: *Nature Methods* 9.7 (July 2012), pp. 676–682. ISSN: 1548-7091, 1548-7105. DOI: 10.1038/nmeth.2019.

[41] Dan E. Midgett, Mary E. Pease, Joan L. Jefferys, Mohak Patel, Christian Franck, Harry A. Quigley, and Thao D. Nguyen. "The pressure-induced deformation response of the human lamina cribrosa: Analysis of regional variations". en. In: *Acta Biomaterialia* 53 (Apr. 2017), pp. 123–139. ISSN: 17427061. DOI: 10.1016/j.actbio.2016.12.054.

[42] Jost B. Jonas and Leonard Holbach. "Central Corneal Thickness and Thickness of the Lamina Cribrosa in Human Eyes". en. In: *Investigative Opthalmology Visual Science* 46.4 (Apr. 1, 2005), p. 1275. ISSN: 1552-5783. DOI: 10.1167/iovs.04-0851.

[43] E. Bar-Kochba, J. Toyjanova, E. Andrews, K.-S. Kim, and C. Franck. "A Fast Iterative Digital Volume Correlation Algorithm for Large Deformations". en. In: *Experimental Mechanics* 55.1 (Jan. 2015), pp. 261–274. ISSN: 0014-4851, 1741-2765. DOI: 10.1007/s11340-014-9874-2.

[44] Nick McCormick and Jerry Lord. "Digital Image Correlation". en. In: *Materials Today* 13.12 (Dec. 2010), pp. 52–54. ISSN: 13697021. DOI: 10.1016/S1369-7021(10)70235-2.

[45] D. Lecompte, A. Smits, Sven Bossuyt, H. Sol, J. Vantomme, D. Van Hemelrijck, and A.M. Habraken. "Quality assessment of speckle patterns for digital image correlation". en. In: *Optics and Lasers in Engineering* 44.11 (Nov. 2006), pp. 1132–1145. ISSN: 01438166. DOI: 10.1016/j.optlaseng.2005.10.004.

[46] Baptiste Coudrillier, Ian C. Campbell, A. Thomas Read, Diogo M. Geraldes, Nghia T. Vo, Andrew Feola, John Mulvihill, Julie Albon, Richard L. Abel, and C. Ross Ethier. "Effects of Peripapillary Scleral Stiffening on the Deformation of the Lamina Cribrosa". en. In: *Investigative Opthalmology Visual Science* 57.6 (May 16, 2016), p. 2666. ISSN: 1552-5783. DOI: 10.1167/iovs.15-18193.

[47] Andrew J. Feola, Baptiste Coudrillier, John Mulvihill, Diogo M. Geraldes, Nghia T. Vo, Julie Albon, Richard L. Abel, Brian C. Samuels, and C. Ross Ethier. "Deformation of the Lamina Cribrosa and Optic Nerve Due to Changes in Cerebrospinal Fluid Pressure". en. In: *Investigative Opthalmology Visual Science* 58.4 (Apr. 7, 2017), p. 2070. ISSN: 1552-5783. DOI: 10.1167/iovs.16-21393.

[48] Arina Korneva, Elizabeth C. Kimball, Joan L. Jefferys, Harry A. Quigley, and Thao D. Nguyen. "Biomechanics of the optic nerve head and peripapillary sclera in a mouse model of glaucoma". en. In: *Journal of The Royal Society Interface* 17.173 (Dec. 2020), p. 20200708. ISSN: 1742-5689, 1742-5662. DOI: 10.1098/rsif.2020.0708.

[49] M. Baconnais, J. Réthoré, and M. François. "Improvement of the digital image correlation close to the borders of an object". en. In: *Strain* 56.3 (June 2020). [Online; accessed 2022-06-24]. ISSN: 0039-2103, 1475-1305. DOI: 10.1111/str.12340. URL: https://onlinelibrary.wiley.com/doi/10.1111/str.12340.

[50] Yaofeng Sun, John H. L. Pang, Chee Khuen Wong, and Fei Su. "Finite element formulation for a digital image correlation method". en. In: *Applied Optics* 44.34 (Dec. 1, 2005), p. 7357. ISSN: 0003-6935, 1539-4522. DOI: 10.1364/AO.44.007357.

[51] Gail F. Schwartz and Harry A. Quigley. "Adherence and Persistence with Glaucoma Therapy". en. In: *Survey of Ophthalmology* 53.6 (Nov. 2008), S57–S68. ISSN: 00396257. DOI: 10.1016/j.survophthal.2008.08.002.